M, Yoshikawa K, Nishikawa S, Nakatsuji N: Generation of dopaminergic neurons and pigmented epithelia from primate ES cells by stromal cell-derived inducing activity. Proc Natl Acad Sci USA 99 (3): 1580–1585, 2002.

71) Brederlau A, Correia A S, Anisimov S V, Elmi M, Paul G, Roybon L, Morizane A, Bergquist F, Riebe I, Nannmark U, Carta M, Hanse E, Takahashi J, Sasai Y, Funa K, Brundin P, Eriksson P S, Li J Y: Transplantation of human embryonic stem cell-derived cells to a rat model of Parkinson's disease: effect of *in vitro* differentiation on graft survival and teratoma formation. Stem Cells 24 (6): 1433–1440, 2006.

72) Buytaert-Hoefen K A, Alvarez E, Freed C R: Generation of tyrosine hydroxylase positive neurons from human embryonic stem cells after coculture with cellular substrates and exposure to GDNF. Stem Cells 22 (5): 669–674, 2004.

73) Ooto S, Haruta M, Honda Y, Kawasaki H, Sasai Y, Takahashi M: Induction of the differentiation of lentoids from primate embryonic stem cells. Invest Ophthalmol Vis Sci 44 (6): 2689–2693, 2003.

74) Nishida K, Kawasaki S, Adachi W, Kinoshita S: Apolipoprotein J expression in human ocular surface epithelium. Invest Ophthalmol Vis Sci 37 (11): 2285–2292, 1996.

75) Munier F L, Korvatska E, Djemai A, Le Paslier D, Zografos L, Pescia G, Schorderet D F: Kerato-epithelin mutations in four 5q31-linked corneal dystrophies. Nat Genet 15 (3): 247–251, 1997.

76) Pellegrini G, Dellambra E, Golisano O, Martinelli E, Fantozzi I, Bondanza S, Ponzin D, McKeon F, De Luca M: p63 identifies keratinocyte stem cells. Proc Natl Acad Sci USA 98 (6): 3156–3161, 2001.

77) Watanabe K, Nishida K, Yamato M, Umemoto T, Sumide T, Yamamoto K, Maeda N, Watanabe H, Okano T, Tano Y: Human limbal epithelium contains side population cells expressing the ATP-binding cassette transporter ABCG2. FEBS Lett 565 (1–3): 6–10, 2004.

78) Yang A, Kaghad M, Wang Y, Gillett E, Fleming M D, Dotsch V, Andrews N C, Caput D, McKeon F: p63, a p53 homolog at 3q27–29, encodes multiple products with transactivating, death-inducing, and dominant-negative activities. Mol Cell 2 (3): 305–316, 1998.

79) Yang A, Schweitzer R, Sun D, Kaghad M, Walker N, Bronson R T, Tabin C, Sharpe A, Caput D, Crum C, McKeon F: p63 is essential for regenerative proliferation in limb, craniofacial and epithelial development. Nature 398 (6729): 714–718, 1999.

80) Kawasaki S, Tanioka H, Yamasaki K, Connon C J, Kinoshita S: Expression and tissue distribution of p63 isoforms in human ocular surface epithelia. Exp Eye Res 82 (2): 293–299, 2006.

81) Kawasaki S, Tanioka H, Yamasaki K, Yokoi N, Komuro A, Kinoshita S: Clusters of corneal epithelial cells reside ectopically in human conjunctival epithelium. Invest Ophthalmol Vis Sci 47 (4): 1359–1367, 2006.

82) Tanioka H, Kawasaki S, Yamasaki K, Ang L P, Koizumi N, Nakamura T, Yokoi N, Komuro A, Inatomi T, Kinoshita S: Establishment of a cultivated human conjunctival epithelium as an alternative tissue source for autologous corneal epithelial transplantation. Invest Ophthalmol Vis Sci 47: 3820–3827, 2006.

83) Sekiyama E, Nakamura T, Kawasaki S, Sogabe H, Kinoshita S: Different expression of angiogenesis-related factors between human cultivated corneal and oral epithelial sheets. Exp Eye Res 83: 741–746, 2006.

84) Sekiyama E, Nakamura T, Cooper L J, Kawasaki S, Hamuro J, Fullwood N J, Kinoshita S: Unique distribution of thrombospondin-1 in human ocular surface epithelium. Invest Ophthalmol Vis Sci 47 (4): 1352–1358, 2006.

85) Ueta M, Nochi T, Jang M H, Park E J, Igarashi O, Hino A, Kawasaki S, Shikina T, Hiroi T, Kinoshita S, Kiyono H: Intracellularly expressed TLR2s and TLR4s contribution to an immunosilent environment at the ocular mucosal epithelium. J Immunol 173 (5): 3337–3347, 2004.

86) Takeda K, Kaisho T, Akira S: Toll-like receptors. Annu Rev Immunol 21: 335–376, 2003.

87) Hozono Y, Ueta M, Hamuro J, et al: Human corneal epithelial cells respond to ocular-pathogenic, but not to nonpathogenic-flagellin. Biochem Biophys Res Commun 347 (1): 238-247, 2006.
88) Ueta M, Hamuro J, Kiyono H, Kinoshita S: Triggering of TLR3 by polyI:C in human corneal epithelial cells to induce inflammatory cytokines. Biochem Biophys Res Commun 331 (1): 285-294, 2005.
89) Kawasaki S, Nishida K, Sotozono C, Quantock A J, Kinoshita S: Conjunctival inflammation in the chronic phase of Stevens-Johnson syndrome. Br J Ophthalmol 84 (10): 1191-1193, 2000.
90) Nakamura T, Nishida K, Dota A, Matsuki M, Yamanishi K, Kinoshita S: Elevated expression of transglutaminase 1 and keratinization-related proteins in conjunctiva in severe ocular surface disease. Invest Ophthalmol Vis Sci 42 (3): 549-556, 2001.
91) Sotozono C, Ang L P K, Koizumi N, Higashihara H, Ueta M, Inatomi T, Yokoi N, Kaido M, Dogru M, Shimazaki J Tsubota K, Yamada M, Kinoshita S: A new grading system for the evaluation of chronic ocular manifestations in patients with Stevens-Johnson syndrome. Ophthalmology. (in press)
92) Ueta M, Hamuro J, Yamamoto M, Kaseda K, Akira S, Kinoshita S: Spontaneous ocular surface inflammation and goblet cell disappearance in I kappa B zeta gene-disrupted mice. Invest Ophthalmol Vis Sci 46 (2): 579-588, 2005.

Strategic Research and Development of Novel Therapeutic Modalities for Ocular Surface Diseases by Regenerative Medicine

Shigeru Kinoshita[1], Chie Sotozono[1], Tsutomu Inatomi[1], Takahiro Nakamura[2], Noriko Koizumi[2], Satoshi Kawasaki[1], Mayumi Ueta[1], Norihiko Yokoi[1], Morio Ueno[1,3], Yoshiki Sasai[3]

[1] Department of Ophthalmology, Kyoto Prefectural University of Medicine
[2] Research Center for Regenerative Medicine, Doshisha University
[3] Organogenesis and Neurogenesis Group, RIKEN Center for Developmental Biology

Journal of Dermatological Science (2006) 42, 111–119

ELSEVIER

Dermatological SCIENCE

www.intl.elsevierhealth.com/journals/jods

Bone morphogenetic protein-2 modulates Wnt and frizzled expression and enhances the canonical pathway of Wnt signaling in normal keratinocytes

Lujun Yang, Kenshi Yamasaki, Yuji Shirakata *, Xiuju Dai, Sho Tokumaru, Yoko Yahata, Mikiko Tohyama, Yasushi Hanakawa, Koji Sayama, Koji Hashimoto

Department of Dermatology, Ehime University School of Medicine, Shitsukawa, Toon, Ehime 791-0295, Japan

Received 21 July 2005; received in revised form 6 December 2005; accepted 19 December 2005

KEYWORDS
BMP-2;
Frizzled;
Keratinocyte;
TCF/LEF;
Wnt

Summary

Background: Bone morphogenetic protein-2 (BMP-2) and Wnt are involved in the normal development and tumorigenesis of several organs, and in the development of skin and skin appendages as a morphogen. However, the crosstalk between BMP-2 and the Wnt/β-catenin signaling pathway is not clear.
Objective: We examined BMP-2-dependent expression of Wnt and its receptor frizzled in normal human keratinocytes.
Methods: The mRNA expression of the Wnt and frizzled families was analyzed by reverse transcription-polymerase chain reaction (RT-PCR) or ribonuclease protection assay. β-Catenin expression was measured using RT-PCR and Western blotting. T-cell factor/lymphoid enhancing factor activity was analyzed using the luciferase reporter assay.
Results: We detected the expression of Wnt-2b/13, -4, -5a, -5b, -7a, -7b, and -10a, frizzled-1, -4, -5, -6, -8, -9, and -10, MFRP, and SFRP-1/SARP-2 in keratinocytes. BMP-2 increased Wnt-2b/13, -5b, and -7b, and frizzled-6, -8, and -10. Conversely, BMP-2 suppressed Wnt-10a and SFRP-1/SARP-2. Although Wnt-4 expression was not affected by BMP-2 in confluent conditioned keratinocytes, BMP-2 suppressed cell density-dependent Wnt-4 induction. The transcriptional activity of TCF/LEF, which is a target of the canonical Wnt pathway, was upregulated by BMP-2 in both time- and dose-

Abbreviations: BHE, bovine hypothalamic extract; BMP, bone morphogenetic protein; GAPDH, glyceraldehyde-3-phosphate dehydrogenase; GSK-3β, glycogen synthase kinase-3; MFRP, membrane-type frizzled-related protein; SARP, secreted apoptosis-related protein; SFRP, secreted frizzled-related protein; TCF/LEF, T-cell factor/lymphoid enhancing factor

* Corresponding author. Tel.: +81 89 960 5350; fax: +81 89 960 5352.
E-mail address: shirakat@m.ehime-u.ac.jp (Y. Shirakata).

0923-1811/$30.00 © 2005 Japanese Society for Investigative Dermatology. Published by Elsevier Ireland Ltd. All rights reserved.
doi:10.1016/j.jdermsci.2005.12.011

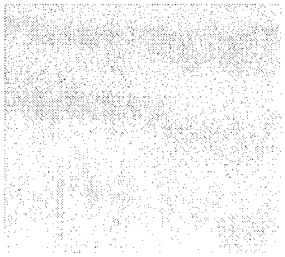

dependent manners. However, BMP-2-dependent differentiation of keratinocytes suppressed TCF/LEF transcriptional activity.
Conclusion: These results suggest that BMP-2 modulates the expression of molecules involved in Wnt signaling, and activates the canonical Wnt pathway in normal human keratinocytes. Moreover, Wnt signaling may be influenced by the fate of keratinocytes, such as proliferation, migration, and differentiation.
© 2005 Japanese Society for Investigative Dermatology. Published by Elsevier Ireland Ltd. All rights reserved.

1. Introduction

The Wnt family is a major gene family that is expressed in developing organs. Wnt genes encode secreted glycoproteins, and Wnt signals are involved in embryonic development, the generation of cell polarity, and the specification of cell fate [1]. Nineteen Wnt genes have been identified in humans [2], and at least four Wnt signaling pathways have been elucidated: the β-catenin pathway (canonical Wnt pathway), which activates target genes in the nucleus; the planar cell polarity pathway, which involves JNK (jun N-terminal kinase) and cytoskeletal rearrangements; the Wnt/Ca^{2+} pathway, which involves activation of PLC and PKC; and the pathway that regulates spindle orientation and asymmetric cell division [3]. Of these, the β-catenin pathway is essential for Wnt function, and has been studied intensely.

In the canonical pathway of Wnt signaling, Wnt transmits signals by binding to frizzled cell-surface receptors. Ten frizzled members have been identified in humans. Frizzled has seven transmembrane domains, a short cytoplasmic tail containing a consensus PSD-95/Dlg/ZO-1 homology (PDZ) domain-binding motif at the carboxyl terminus, and an amino-terminal cysteine-rich domain that binds Wnt [2]. Frizzled activates Disheveled, which inactivates glycogen synthase kinase-3β (GSK-3β), and saves β-catenin from ubiquitination and degradation [4]. Stabilized β-catenin accumulates in the cytoplasm and translocates to the nucleus, where it binds transcription factors of the T-cell factor/lymphoid enhancing factor (TCF/LEF) family, and activates the transcription of target genes, such as c-myc, cyclin D1, and c-jun, which are involved in carcinogenesis [3,5]. The Wnt/β-catenin signaling pathway has important roles in tumorigenesis and in the differentiation and patterning of diverse tissues during animal development [2]. Moreover, roles in the development of skin, hair, and related appendages have been suggested. For example, Wnt-3a and -7a can act as inductive signals to maintain dermal papillae in an anagen state [6]. Wnt-4 proteins are thought to be involved in epidermal–dermal interactions in mammalian skin [7]. The expression of mouse frizzled-3 is reported to be restricted to the epidermis and developing hair follicles, and a role in follicle development has been suggested [8].

Despite many studies of Wnt expression and its roles in animal skin, the factors and mechanisms that regulate the Wnt/β-catenin signaling pathway in skin are poorly understood. In epithelial–mesenchymal interactions in the initial morphogenesis of the mammalian tooth, both BMP and Wnt signaling activate Lef1 [9]. In cultured murine multipotent mesenchymal cell line C3H10T1/2, BMP-2 upregulates Wnt-3a expression and downregulates Wnt-7a expression [10]. BMP-2 is involved in tissue and organ development and in regulating epidermal induction and keratinocyte differentiation [11]. These data suggest that there is crosstalk between the BMP-2 and Wnt/β-catenin signals in human keratinocytes. In this report, we show that BMP-2 modulates the expression of the Wnt and frizzled families, and enhances the canonical pathway of Wnt signaling in normal human keratinocytes.

2. Materials and methods

2.1. Cell culture

Normal human keratinocytes from an excised polydactyl finger of 1-year-old boy were cultured in MCDB153 medium supplemented with insulin (5 $\mu g\ mL^{-1}$), hydrocortisone (5×10^{-7} M), ethanolamine (0.1 mM), phosphoethanolamine (0.1 mM), bovine hypothalamic extract (BHE) (50 $\mu g\ mL^{-1}$), and Ca^{2+} (0.1 mM), as described previously [12,13]. Third- to fifth-passage cells were used in all of the experiments. All procedures that involved human subjects received prior approval from the Ethics Committee of Ehime University School of Medicine, Toon, Ehime, Japan, and all subjects provided written informed consent.

2.2. Reagents

Recombinant BMP-2 was a generous gift from Yamanouchi Pharmaceutical (Tokyo, Japan). Anti-β-cate-

nin antibody was purchased from New England Biolabs (Beverly, MA, USA). Conditioned medium of Wnt-3a-expressing mouse fibroblasts L cells (L cells) and neomycin-expressing L cells were kind gifts from S. Takada, Center for Molecular and Developmental Biology, Graduate School of Science, Kyoto University, Kyoto, Japan [14].

2.3. RT-PCR analysis

Total RNA from cultured human keratinocytes was prepared with Isogen (Nippon Gene, Toyama, Japan) and treated with 50 U mL^{-1} of DNase 1 (Clontech Laboratories, Palo Alto, CA, USA) at 37 °C for 30 min to remove any contaminating genomic DNA. Specific primers for human frizzled and Wnt cDNA were generated by selecting specific nucleotide sequences corresponding to the following oligonucleotides (Table 1). Reverse transcription-polymerase chain reaction (RT-PCR) was performed using RT-PCR High Plus™ (Toyobo, Osaka, Japan) according to the manufacturer's instructions. Briefly, 1 μg of total RNA was added to a 50-μL reaction mixture containing 10 μL of 5× reaction buffer, 6 μL of 2.5 mM dNTPs, 5 μL of 25 mM $Mn(OAc)_2$, 19 μL of RNase-free H_2O, 2 μL of 10 U μL^{-1} RNase inhibitor, 2 μL of 2.5 U μL^{-1} of rTth DNA polymerase, and 2 μL of 10 pmol μL^{-1} of each primer. cDNA was reverse transcribed from total RNA for 30 min at 60 °C, and heated to 94 °C for 2 min. Amplification was performed using a DNA thermal cycler (Astec, Fukuoka, Japan) for 25–38 cycles. The cycle profile consisted of 1 min at 94 °C for denaturation, and 1.5 min at 60 °C for annealing and primer extension. To evaluate the amplification, 5 μL of the reaction mixture was electrophoresed on a 2.0% agarose gel containing ethidium bromide. The PCR products were sequenced to confirm the amplification. We performed at least three independent studies and confirmed similar results. A representative experiment is shown in the figures.

2.4. Oligonucleotide probe preparation

PCR amplified human cDNAs were inserted into the *Eco*RI and *Hin*dIII sites of the pPMG vector (PharMingen, San Diego, USA). The inserted cDNAs corresponded to the oligonucleotides described above. These inserted cDNAs were confirmed by nucleotide sequencing. The pPMG vector, including GAPDH cDNA (PharMingen), was used as the internal standard. We used the hFrizzled RPA templates set (PharMingen) to detect frizzled-2 to -6 and SFRP-1 and -2.

2.5. Ribonuclease protection assay

Single-stranded antisense riboprobes were prepared by in vitro transcription of human cDNA fragments, using the RiboQuant® In Vitro Transcription kit (PharMingen) in the presence of [α-^{32}P] UTP. Samples of total RNA (10 μg each) were hybridized with ^{32}P-labeled riboprobe, and digested with RNase using the RiboQuant® RPA kit (PharMingen) according to the manufacturer's instructions. The hybridization products were separated on a gel and exposed to a film, as described previously [15]. We performed at least three independent studies and confirmed similar results. A representative experiment is shown in the figures.

2.6. Western blot analysis

For total cellular protein extraction, cells were harvested by scraping with extraction buffer con-

Table 1. sequence and accession number for primers

Primers for	Sequence	Accession number	Primers for	Sequence	Accession number
Frizzled-1	1247–1561	AF072872	Wnt-4	683–874	AF316543
Frizzled-4	1373–1651	AB032471	Wnt-5a	594–770	L20861
Frizzled-7	726–956	BC015915	Wnt-5b	76–232	AB060966
Frizzled-8	748–964	AB043703	Wnt-6	399–540	NM006522
Frizzled-9	1253–1444	U82169	Wnt-7a	595–722	U53476
Frizzled-10	1571–1746	AB027464	Wnt-7b	19–126	AF062766
SFRP (secreted frizzled-related protein)-4	775–929	E288952	Wnt-8a	107–427	AB057725
SFRP-5/secreted apoptosis-related (SARP)	686–825	AF117758	Wnt-8b	176–456	NM003393
Membrane-type frizzled-related protein (MFRP)	1008–1128	AB055505	Wnt-10a	317–574	AY009400
Wnt-1	325–650	NM005430	Wnt-10b/12	848–1081	NM003394
Wnt-2	373–665	X07876	Wnt-11	678–877	Y12692
Wnt-2b/13	1318–1487	Z71621	—	884–1032	NM003395
Wnt-3	385–636	NM0307	Wnt-14b/15	283–412	AB063483
Wnt-3a	10–231	XM047539	Wnt-16	661–773	AF152584

taining 150 mM NaCl, 1% Nonidet P-40, 0.5% deoxycholate, 0.1% SDS, 50 mM Tris–HCl pH 7.4, and protease inhibitors, and sonicated on ice. Equal amounts of protein (2.5 μg/lane) were separated by sodium dodecyl sulfate-polyacrylamide gel electrophoresis (SDS-PAGE), and transferred to polyvinylidene difluoride membranes. The first antibodies were incubated overnight at 4 °C. The analysis was performed using the Vistra ECF kit (Amersham Biosciences K.K., Tokyo, Japan) and Fluoroimager (Molecular Dynamics, Sunnyvale, CA), as described previously [15]. We performed at least three independent studies and confirmed similar results. A representative experiment is shown in the figures.

2.7. Luciferase reporter assay

Keratinocytes were seeded at 4.0×10^4 cells per well in 12-well collagen-coated dishes (Iwaki Glass, Tokyo, Japan), and cultured in 1 mL of MCDB153 medium with BHE. The medium was replaced 48 h later with 1 mL of fresh MCDB153 without BHE, with 0.5 μg of TOPFLASH containing three copies of the TCF/LEF consensus sequence or FOPFLASH containing three copies of a mutated consensus sequence, and 10 ng of pRL-CMV (Promega, Madison, WI, USA) as an internal standard of transfection. The keratinocytes were transfected using FUGENE6™ (Roche Diagnostic, Tokyo, Japan) according to the manufacturer's instructions. After a 10-h transfection with the reporter gene, the medium was replaced with 1 mL of fresh MCDB153 without BHE, and various concentrations of BMP-2 or conditioned medium of Wnt-3a-expressing L cells were added (keratinocyes were subconfluent). The cells were harvested 72 h later (keratinocyes reached confluency), and luciferase activity was measured using the Dual-Luciferase Reporter Assay System (Promega) according to the manufacturer's instructions. The transfection efficiency was standardized using an internal control, pRL-CMV. The mean and standard deviation of the relative values obtained from three independent experiments were plotted on graphs. Statistical analysis was performed using Student's *t*-test.

3. Results

3.1. BMP-2 enhances Wnt and frizzled gene expression in normal human keratinocytes

To explore the effects of BMP-2 on the expression of Wnt and frizzled family members in human keratinocytes, we stimulated quiescent (confluent conditioned) normal human keratinocytes with BMP-2 and examined Wnt and frizzled mRNA expression. Expression of the 19 Wnt family members (Wnt-1, -2, -2b/13, -3, -3a, -4, -5a, -5b, -6, -7a, -7b, -8a, -8b, -10a, -10b, -11, -14, -14b/15, and -16) in normal

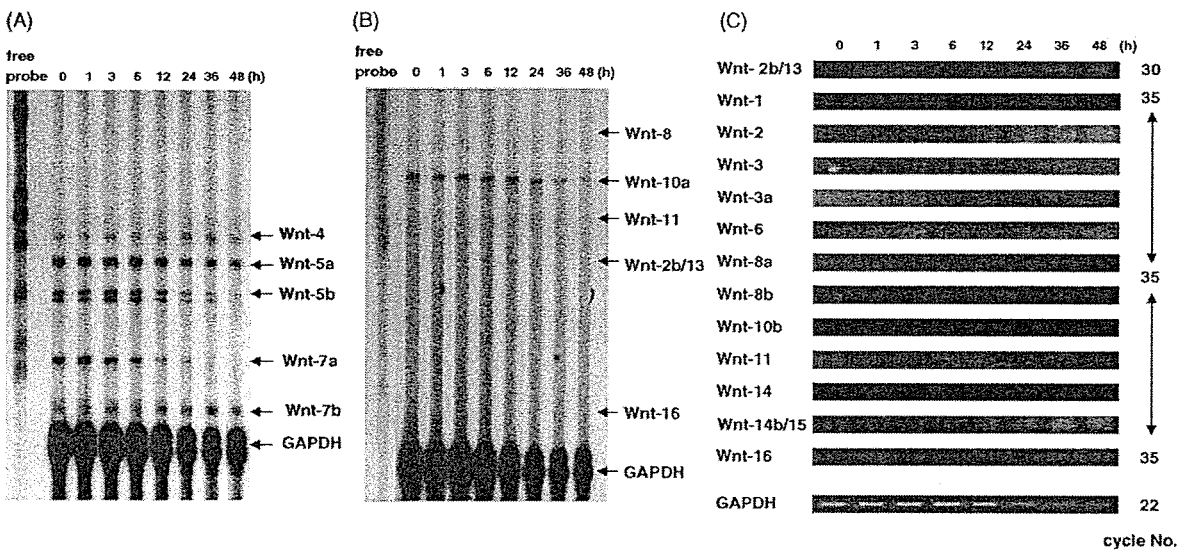

Fig. 1 BMP-2 modulates Wnt mRNA expression. (A and B) Keratinocytes were seeded and cultured until they reached subconfluence. After changing the medium to BHE-free MCDB153, the keratinocytes were cultured for a further 24 h. BMP-2 (4 ng mL^{-1}) was added to the keratinocyte culture medium, and total RNA was extracted 0, 1, 3, 6, 12, 24, 36, and 48 h after stimulation. Total RNA was hybridized with RNA probes, and separated on a polyacrylamide gel. GAPDH is the control mRNA. Three independent experiments were performed, and a representative experiment is shown. (C) Keratinocytes were stimulated, and total RNA was extracted as described above. Total RNA was used for RT-PCR, with the primers indicated to the left of the panel, and the cycle numbers indicated to the right. GAPDH was the control mRNA.

human epidermal keratinocytes was examined using a ribonuclease protection assay and RT-PCR. Of the Wnt family, Wnt-2b/13, -4, -5a, -5b, -7a, -7b, and -10a mRNAs were detected, while the other Wnt mRNAs were not (Fig. 1A–C). The expression of Wnt-2b/13 mRNA was upregulated beginning 24 h post-BMP-2 stimulation, and increased in a time-dependent manner (Fig. 1C). BMP-2 did not influence the expression of Wnt-4, -5a, and -7b mRNA (Fig. 1A). Wnt-10a decreased beginning 36 h post-BMP-2 stimulation (Fig. 1B). Wnt-5b increased transiently from 1 to 6 h, and decreased after 12 h (Fig. 1A). Wnt-7a mRNA increased transiently at 1 h, returned to the basal level at 3 h, decreased after 12 h, and was hardly detected after 36 h (Fig. 1A).

Next, we examined the expression of frizzled and related genes (frizzled-1, -2, -3, -4, -4s, -5, -6, -7, -8, -9, and -10, SFRP-1/SARP-2, SFRP-2/SARP-1, SFRP-4, SFRP-5/SARP-3, MFRP, and smoothened) using a ribonuclease protection assay and RT-PCR. We detected frizzled-5, -6, and SFRP-1/SARP-2 mRNA with the ribonuclease protection assay (Fig. 2A), and frizzled-1, -4, -8, -9, and -10, and membrane-type frizzled-related protein (MFRP) mRNA by RT-PCR (Fig. 2B). Although BMP-2 did not change the expression of frizzled-1, -4, -5, and -9, or MFRP mRNA, it upregulated frizzled-6 and -8 mRNA expression. Frizzled-6 expression increased beginning 6 h post-BMP-2 in a time-dependent manner. Frizzled-8 expression increased transiently from 3 to 24 h, and returned to the basal level by 36 h post-BMP-2. Frizzled-10 expression increased transiently from 3 to 12 h, and returned to the basal level by 36 h post-BMP-2. Interestingly, expression of one of the Wnt signal inhibitors, SFRP-1/SARP-2, decreased beginning 24 h post-BMP-2 in a time-dependent manner (Fig. 2A).

A previous report showed that the Wnt-4 mRNA level increased as normal murine keratinocytes approached confluence [7]. Therefore, we examined Wnt mRNA expression in the subconfluent to confluent condition (Fig. 3). We cultured keratinocytes and stimulated them with BMP-2 or vehicle at a cell density of 50%, and collected total mRNA at the indicated times. The final cell density 48 h post-BMP-2 stimulation was nearly confluent. Wnt-4 expression was upregulated when human keratinocytes reached confluence, as previously reported. Interestingly, BMP-2 suppressed cell density-dependent Wnt-4 induction. The level of Wnt-5a gene expression increased with the confluence of cultured cells of human mammary epithelial cell line HB2 [16]. In contrast, Wnt-5a expression was not

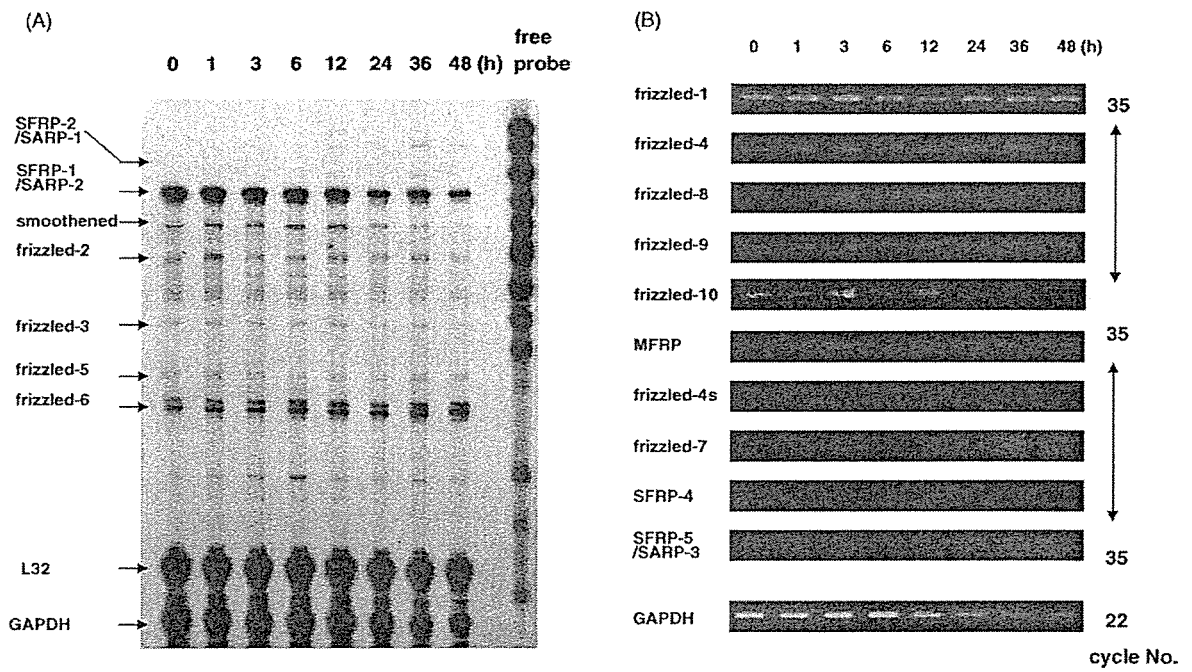

Fig. 2 BMP-2 modulates frizzled mRNA expression. (A) Keratinocytes were cultured and stimulated, and total RNA was extracted as described in the legend of Fig. 1A. Total RNA was hybridized with RNA probes, and separated on a polyacrylamide gel. L32 and GAPDH were the internal standards. (B) Keratinocytes were cultured and stimulated, and total RNA was extracted as described above and used for RT-PCR. The primers used are indicated to the left, and the cycle numbers to the right. GAPDH was the control mRNA.

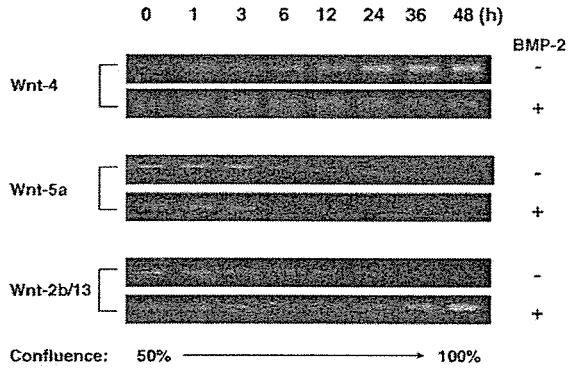

Fig. 3 BMP-2 increased Wnt-13 and decreased Wnt-4 mRNA expression. Keratinocytes were seeded and cultured until they reached 30–40% confluence. After changing the medium to BHE-free MCDB153, keratinocytes were cultured for a further 24 h. At this time, the keratinocytes reached about 50% confluence. BMP-2 (4 ng mL^{-1}) or vehicle was added to the keratinocyte culture medium, and total RNA was extracted 0, 1, 3, 6, 12, 24, 36, and 48 h after stimulation. The expression of Wnt-4, -5a, and -2b/13 was analyzed by RT-PCR.

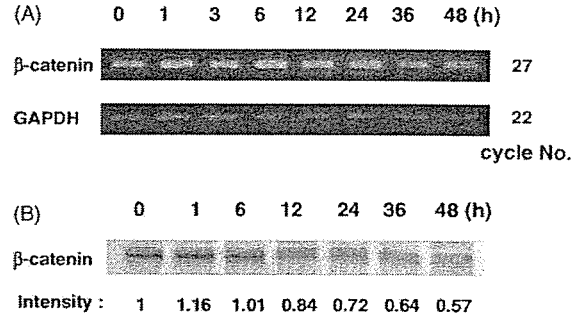

Fig. 4 BMP-2 did not enhance β-catenin expression. (A) BMP-2 (4 ng mL^{-1}) was added to the keratinocyte culture medium, and total RNA was extracted at indicated time points. The expression of β-catenin was analyzed by RT-PCR. (B) BMP-2 (4 ng mL^{-1}) was added to the keratinocyte culture medium, and cellular protein was extracted. Western blot analyses were performed with anti-β-catenin antibody. The intensity of each band was quantified, referring to the signal of the 0-h sample as 1 unit, and the mean of three independent studies is indicated.

enhanced with increasing cell density in human epidermal keratinocytes, and BMP-2 did not affect the cell density-dependent Wnt-5a expression pattern. Wnt-2b/13 decreased in a cell density-dependent manner, and BMP-2 increased Wnt-2b/13 expression in the confluent condition.

3.2. Effects of BMP-2 on β-catenin and TCF/LEF transcriptional activity

β-Catenin and TCF/LEF transcription factors are downstream targets of the Wnt canonical signaling pathway. Endogenous β-catenin activates TCF/LEF transcription activity [17]. We found that BMP-2 upregulated the expression of several Wnt and frizzled mRNAs. Therefore, we examined whether BMP-2 activates β-catenin for TCF/LEF signaling in human keratinocytes.

First, we examined the expression of β-catenin mRNA and protein in keratinocytes. BMP-2 did not change the expression of β-catenin mRNA (Fig. 4A). β-Catenin protein was transiently increased 1 h post-BMP-2 stimulation, returned to the basal level at 6 h, and then decreased in a time-dependent manner (Fig. 4B).

We then performed luciferase assays to examine TCF/LEF transcription activity. First, we examined TCF/LEF activity in keratinocytes using exogenous Wnt. We used conditioned medium of Wnt-3a-expressing L cells because Wnt-3a activates the canonical pathway [14]. Keratinocytes did not express Wnt-3a mRNA (Fig. 1C), so we did not need to consider the effect of intrinsic Wnt-3a. Keratinocytes were transfected with TOPFLASH, and then stimulated with Wnt-3a for 48 h. Wnt-3a increased the luciferase activity 6.3-fold compared with unstimulated keratinocytes, while control medium (conditioned medium of neomycin-expressing L cells) did not increase the luciferase activity (Fig. 5A). Next, we examined the effects of BMP-2 on TCF/LEF activity. Keratinocytes were transfected with TOPFLASH or FOPFLASH, and then stimulated with BMP-2 for 48 h. Luciferase activity was very low in FOPFLASH-transfected cells, and remained unchanged with BMP-2 (Fig. 5B). TOPFLASH activity in keratinocytes was significantly elevated with BMP-2 relative to the basal level. Upregulation occurred in both time- and dose-dependent manners (Fig. 5B and C). The presence of 2 ng mL^{-1} BMP-2 increased the TOPFLASH luciferase activity 2-fold, and 4 ng mL^{-1} increased it 3.5-fold relative to the basal level. However, 10 ng mL^{-1} BMP-2 only increased TOPFLASH luciferase activity 1.4-fold; because 10 ng mL^{-1} BMP-2 also induced striking morphological changes (stratification and enlargement) in cultured cells after a 48-h stimulation (unpublished data), the reduced luciferase activity is thought to result from keratinocyte differentiation. The combination of BMP-2 and Wnt-3a induced more transcription than did either BMP-2 or Wnt-3a alone (Fig. 5D). Therefore, BMP-2 enhanced TOPFLASH transcription synergistically with Wnt-3a, which suggests that BMP-2 modulates Wnt and frizzled expression, and enhances the canonical pathway of Wnt signaling.

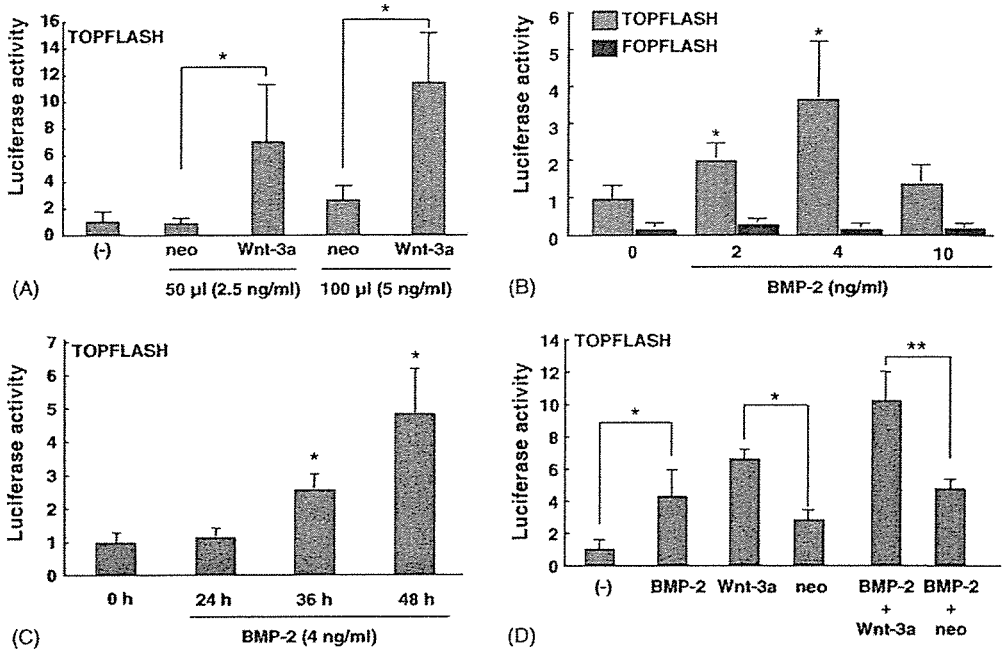

Fig. 5 BMP-2 enhances the canonical Wnt signal pathway. (A) Keratinocytes were seeded at 4.0×10^4 per well in 12-well collagen-coated dishes, and cultured in 1 mL of MCDB153 medium with BHE. After 48 h, the medium was replaced with 1 mL of fresh MCDB153 without BHE, and 0.5 μg of TOPFLASH and 10 ng of pRL-CMV were transfected. After a 10-h transfection of the reporter gene, the medium was replaced with 1 mL of fresh MCDB153 without BHE. Various concentrations of conditioned medium of L cells that expressed the Wnt-3a gene or neomycin (control vector) were added to the medium, and the cells were incubated for 72 h. Cells were harvested, and luciferase activity was measured. The luciferase activity of each sample was normalized against that of a non-stimulated sample. (B) Keratinocytes were cultured as described above, and transfected with 0.5 μg of TOPFLASH or FOPFLASH and 10 ng of pRL-CMV. After a 10-h transfection of the reporter gene, the medium was replaced with 1 mL of fresh MCDB153 without BHE. Various concentrations of BMP-2 were added to the medium and the cells were incubated for 72 h. The luciferase activity of each sample was normalized against that of a TOPFLASH-transfected, non-stimulated sample. (C) Keratinocytes were cultured as described above, and transfected with 0.5 μg of TOPFLASH and 10 ng of pRL-CMV. After a 10-h transfection of the reporter gene, the medium was replaced with 1 mL of fresh MCDB153 without BHE. BMP-2 (4 ng mL^{-1}) was added to the medium 24, 36, and 48 h before the cells were harvested, and luciferase activity was measured. The luciferase activity of each sample was normalized against that of a non-stimulated sample. (D) Keratinocytes were cultured as described above, and transfected with 0.5 μg of TOPFLASH and 10 ng of pRL-CMV. After a 10-h transfection of the reporter gene, the medium was replaced with 1 mL of fresh MCDB153 without BHE. BMP-2 (4 ng mL^{-1}) in combination with conditioned medium (5 ng mL^{-1}) of L cells that expressed the Wnt-3a gene or neomycin (control vector) were added to the medium, and the cells were incubated for 72 h. The luciferase activity of each sample was normalized against that of a non-stimulated sample. The bars and error bars represent the mean and S.D. of three independent experiments ($^{*}p < 0.05$ and $^{**}p < 0.01$).

4. Discussion

By definition, both BMP-2 and Wnts are morphogens that specify different cell fates in concentration-dependent manners [18]. BMP-2 could induce epidermal fate of ectodermal cells during embryogenesis, and regulate hair follicle development [19–21]. Several reports revealed the roles of Wnts, Frizzleds, and β-catenin in regulating skin and hair development which suggested Wnt/β-catenin pathway might be involved [22–24]. In our experiment, Wnt-2b/13, -4, -5a, -5b, -7a, -7b, and -10a mRNAs were detected in keratinocytes, and BMP-2 increased Wnt-2b/13, and decreased Wnt-10a. Wnt-5b and -7a increased transiently soon after BMP-2 stimulation, and later decreased (Fig. 1). Interestingly, although BMP-2 did not decrease Wnt-4 expression in the confluent condition, BMP-2 suppressed cell density-dependent Wnt-4 induction (Figs. 1 and 3). In contrast, BMP-2 increased Wnt-2b/13 in both the confluent and sub-confluent conditions (Figs. 1 and 3). These results suggest that BMP-2 modulates Wnt expression in keratinocytes, and cell confluence affects BMP-2-dependent Wnt induction. BMP-2 modulates the expression of Wnt-3a and -7a mRNA, and BMP-2 can upregulate the activity of lef1 in the murine

multipotent mesenchymal cell line C3H10T1/2 [9,10]. In hair budding, however, BMP induces E-cadherin by suppressing Lef1 activation, and the balance between the BMP and Wnt signals regulates proper hair budding [25]. Therefore, cell types and cell conditions, such as proliferation, differentiation, and the cell environment, may influence the interaction between BMP-2 and Wnt.

In the frizzled family, BMP-2 increased frizzled-6 in a time-dependent manner, and transiently increased frizzled-8 and -10 (Fig. 2). These results suggest that BMP-2-treated keratinocytes are susceptible to Wnt stimulation. Interestingly, human keratinocytes express abundant SFRP-1/SARP-2 mRNA, and BMP-2 suppressed SFRP-1/SARP-2 expression (Fig. 2). SFRP/SARP mRNAs encode secreted proteins that possess a cysteine-rich domain homologous to those of frizzled proteins, but lack the transmembrane regions that are characteristic of frizzled-like proteins. It has been suggested that SFRP/SARPs bind to Wnt and interfere with the interaction between Wnt and frizzled, resulting in Wnt signal suppression, because SFRP-1/SARP-2 decreases the intracellular β-catenin concentration in cultured human breast adenocarcinoma MCF7 cells [26]. The increases in frizzled-6, -8, and -10, and the decrease in SFRP-1/SARP-2 by BMP-2 suggest that frizzled-6, -8, and -10, and SFRP-1/SARP-2 enhance the Wnt signaling pathway with BMP-2 stimulation in a coordinated manner.

TCF/LEF members, originally cloned as lymphoid transcription factors, are recognized as potent transactivators on interaction with β-catenin, the downstream target of Wnt signaling [27]. BMP-2 upregulated the transcriptional activity of TCF/LEF in human keratinocytes, and BMP-2 enhanced Wnt-3a-dependent TCF/LEF activation (Fig. 5). BMP-2 upregulated the expression of some members, such as Wnt-2b/13 and frizzled-6, which suggests that these Wnt and frizzled genes are involved in the subsequent activation of TCF/LEF in human keratinocytes. Other mechanisms may also be involved in BMP-2-dependent TCF/LEF activation. The BMP-2 signal is transduced by the smad family, and smad4 interacts with TCF/LEFs directly [28]. Thus, smad4, which is activated by BMP-2 signaling and translocated into the nucleus, may activate TCF/LEF directly, and support Wnt-3a-dependent TCF/LEF activation. At the least, BMP-2 enhanced the canonical Wnt pathway in normal human keratinocytes under certain conditions. However, 10 ng mL^{-1} of BMP-2 did not activate the canonical Wnt pathway (Fig. 5B). This may be the effect of keratinocyte differentiation because 10 ng mL^{-1} of BMP-2 induced morphological changes in some genes that are induced in differentiated keratinocytes (unpublished data). Cell differentiation affects the expression of some Wnt, frizzled, and TCF/LEF genes [7,8,29]. Therefore, strong BMP-2 stimulation induces keratinocyte differentiation, and may not enhance TOPFLASH luciferase activity.

The particular stem cell lineage and stage of differentiation of the skin cell may influence the cell response to Wnt/β-catenin signaling. Mutated β-catenin without transcriptional activity acts in epidermis to promote hair fate and in hair cells to promote epidermal fate [30]; skin stem cells fail to differentiate into follicular KC in the absence of β-catenin, but instead adopt an epidermal fate [22]. In cultured normal human keratinocytes, we showed BMP-2 modulates the expression of molecules related to Wnt signaling and activates the canonical Wnt pathway, and Wnt signaling may be affected by the fate of keratinocytes, such as their proliferation, migration and differentiation. However, the target genes of TCF/LEF activated by BMP-2 in normal human keratinocytes are not clear. It is our future concern to reveal the target genes and the downstream biological/cellular events which might be influenced by these target genes in normal human keratinocytes.

In conclusion, BMP-2 modulates the expression of molecules related to Wnt signaling and activates the canonical Wnt pathway in normal human keratinocytes. Moreover, Wnt signaling may be affected by the fate of keratinocytes, such as their proliferation, migration, and differentiation.

Acknowledgments

This work was partly supported by Health Sciences Research Grants for Research on Specific Diseases from the Ministry of Health, Labor, and Welfare of Japan and a Grant-in-Aid for Scientific Research from the Ministry of Education, Culture, Sports, Science, and Technology of Japan. We thank Teruko Tsuda and Eriko Tan for technical assistance.

References

[1] Cadigan KM, Nusse R. Wnt signaling: a common theme in animal development. Genes Dev 1997;11:3286–305.
[2] Miller JR. The Wnts. Genome Biol 2002;3 [REVIEWS3001, Epub 2001 December 28].
[3] Huelsken J, Birchmeier W. New aspects of Wnt signaling pathways in higher vertebrates. Curr Opin Genet Dev 2001;11:547–53.
[4] van Gijn ME, Snel F, Cleutjens JP, Smits JF, Blankesteijn WM. Overexpression of components of the Frizzled–Dishevelled cascade results in apoptotic cell death, mediated by beta-catenin. Exp Cell Res 2001;265:46–53.

[5] Behrens J. Control of beta-catenin signaling in tumor development. Ann N Y Acad Sci 2000;910:21–33.
[6] Kishimoto J, Burgeson RE, Morgan BA. Wnt signaling maintains the hair-inducing activity of the dermal papilla. Genes Dev 2000;14:1181–5.
[7] Saitoh A, Hansen LA, Vogel JC, Udey MC. Characterization of Wnt gene expression in murine skin: possible involvement of epidermis-derived Wnt-4 in cutaneous epithelial–mesenchymal interactions. Exp Cell Res 1998;243:150–60.
[8] Hung BS, Wang XQ, Cam GR, Rothnagel JA. Characterization of mouse Frizzled-3 expression in hair follicle development and identification of the human homolog in keratinocytes. J Invest Dermatol 2001;116:940–6.
[9] Dassule HR, McMahon AP. Analysis of epithelial–mesenchymal interactions in the initial morphogenesis of the mammalian tooth. Dev Biol 1998;202:215–27.
[10] Fischer L, Boland G, Tuan RS. Wnt signaling during BMP-2 stimulation of mesenchymal chondrogenesis. J Cell Biochem 2002;84:816–31.
[11] Suzuki A, Kaneko E, Ueno N, Hemmati-Brivanlou A. Regulation of epidermal induction by BMP2 and BMP7 signaling. Dev Biol 1997;189:112–22.
[12] Shirakata Y, Tokumaru S, Yamasaki K, Sayama K, Hashimoto K. So-called biological dressing effects of cultured epidermal sheets are mediated by the production of EGF family, TGF-beta and VEGF. J Dermatol Sci 2003;32:209–15.
[13] Shirakata Y, Ueno H, Hanakawa Y, Kameda K, Yamasaki K, Tokumaru S, et al. TGF-beta is not involved in early phase growth inhibition of keratinocytes by 1alpha,25(OH)2Vitamin D3. J Dermatol Sci 2004;36:41–50.
[14] Shibamoto S, Higano K, Takada R, Ito F, Takeichi M, Takada S. Cytoskeletal reorganization by soluble Wnt-3a protein signalling. Genes Cells 1998;3:659–70.
[15] Yamasaki K, Hanakawa Y, Tokumaru S, Shirakata Y, Sayama K, Hanada T, et al. Suppressor of cytokine signaling 1/JAB and suppressor of cytokine signaling 3/cytokine-inducible SH2 containing protein 3 negatively regulate the signal transducers and activators of transcription signaling pathway in normal human epidermal keratinocytes. J Invest Dermatol 2003;120:571–80.
[16] Huguet EL, Smith K, Bicknell R, Harris AL. Regulation of Wnt5a mRNAexpression in human mammary epithelial cells by cell shape, confluence, and hepatocyte growth factor. J Biol Chem 1995;270:12851–6.
[17] Zhu AJ, Watt FM. Beta-catenin signalling modulates proliferative potential of human epidermal keratinocytes independently of intercellular adhesion. Development 1999;126:2285–98.
[18] Christian JL. BMP, Wnt and Hedgehog signals: how far can they go? Curr Opin Cell Biol 2000;12:244–9.
[19] Botchkarev VA, Botchkareva NV, Sharov AA, Funa K, Huber O, Gilchrest BA. Modulation of BMP signaling by noggin is required for induction of the secondary (nontylotrich) hair follicles. J Invest Dermatol 2002;118:3–10.
[20] Qiao W, Li AG, Owens P, Xu X, Wang XJ, Deng CX. Hair follicle defects and squamous cell carcinoma formation in Smad4 conditional knockout mouse skin. Oncogene 2005.
[21] Suzuki A, Kaneko E, Ueno N, Hemmati-Brivanlou A. Regulation of epidermal induction by BMP2 and BMP7 signaling. Dev Biol 1997;189:112–22.
[22] Huelsken J, Vogel R, Erdmann B, Cotsarelis G, Birchmeier W. Beta-catenin controls hair follicle morphogenesis and stem cell differentiation in the skin. Cell 2001;105:533–45.
[23] Reddy S, Andl T, Bagasra A, Lu MM, Epstein DJ, Morrisey EE, et al. Characterization of Wnt gene expression in developing and postnatal hair follicles and identification of Wnt5a as a target of Sonic hedgehog in hair follicle morphogenesis. Mech Dev 2001;107:69–82.
[24] Reddy ST, Andl T, Lu MM, Morrisey EE, Millar SE. Expression of Frizzled genes in developing and postnatal hair follicles. J Invest Dermatol 2004;123:275–82.
[25] Jamora C, DasGupta R, Kocieniewski P, Fuchs E. Links between signal transduction, transcription and adhesion in epithelial bud development. Nature 2003;422:317–22.
[26] Melkonyan HS, Chang WC, Shapiro JP, Mahadevappa M, Fitzpatrick PA, Kiefer MC, et al. SARPs: a family of secreted apoptosis-related proteins. Proc Natl Acad Sci USA 1997;94:13636–41.
[27] Roose J, Clevers H. TCF transcription factors: molecular switches in carcinogenesis. Biochim Biophys Acta 1999;1424:M23–37.
[28] Pukrop T, Gradl D, Henningfeld KA, Knochel W, Wedlich D, Kuhl M. Identification of two regulatory elements within the high mobility group box transcription factor XTCF-4. J Biol Chem 2001;276:8968–78.
[29] Zhou P, Byrne C, Jacobs J, Fuchs E. Lymphoid enhancer factor 1 directs hair follicle patterning and epithelial cell fate. Genes Dev 1995;9:700–13.
[30] DasGupta R, Rhee H, Fuchs E. A developmental conundrum: a stabilized form of beta-catenin lacking the transcriptional activation domain triggers features of hair cell fate in epidermal cells and epidermal cell fate in hair follicle cells. J Cell Biol 2002;158:331–44.

Available online at www.sciencedirect.com
SCIENCE DIRECT®

ORIGINAL ARTICLE

SOCS1-Negative Feedback of STAT1 Activation Is a Key Pathway in the dsRNA-Induced Innate Immune Response of Human Keratinocytes

Xiuju Dai[1], Koji Sayama[1], Kenshi Yamasaki[1], Mikiko Tohyama[1], Yuji Shirakata[1], Yasushi Hanakawa[1], Sho Tokumaru[1], Yoko Yahata[1], Lujun Yang[1], Akihiko Yoshimura[2] and Koji Hashimoto[1]

Toll-like receptor (TLR)3 is a receptor for virus-associated double-stranded RNA, and triggers antiviral immune responses during viral infection. Epidermal keratinocytes express TLR3 and provide an innate immune defense against viral infection. Since the intracellular regulatory mechanism is unknown, we hypothesized that the signal transducers and activators of transcription (STAT)–suppressors of cytokine signaling (SOCS) system regulates the innate immune response of keratinocytes. Treatment with polyinosinic–polycytidylic acid (poly(I:C)) resulted in the rapid translocation of IFN regulatory factor (IRF)-3 into the nucleus, followed by phosphorylation of STAT1 and STAT3. The activation of STATs by poly(I:C) probably occurs in an indirect fashion, through poly(I:C)-induced IFN. We infected cells with the dominant-negative forms of STAT1 (STAT1F), STAT3 (STAT3F), and SOCS1 using adenovirus vectors. Infection with STAT1F suppressed the induction of macrophage inflammatory protein (MIP)-1α by poly(I:C), whereas STAT3F had a minimal effect, which indicates that STAT1 mediates MIP-1α induction. SOCS1, which is a negative feedback regulator of STAT1 signaling, was induced by treatment with poly(I:C). SOCS1 infection inhibited the phosphorylation of STAT1 and significantly reduced poly(I:C)-induced MIP-1α production. Furthermore, STAT1–SOCS1 regulated poly(I:C)-induced TLR3 and IRF-7 expression. However, SOCS1 did not affect NF-κB signaling. Thus, the STAT1–SOCS1 pathway regulates the innate immune response via TLR3 signaling in epidermal keratinocytes.

Journal of Investigative Dermatology (2006) **126,** 1574–1581. doi:10.1038/sj.jid.5700294; published online 20 April 2006

INTRODUCTION

Toll-like receptors (TLRs) play critical roles in innate and adaptive immunity by detecting microbial pathogens. These signals are classified into MyD88-dependent and MyD88-independent pathways, which lead to the transcription of appropriate host-defense genes (Takeda *et al.*, 2003). TLR3 is a receptor for virus-associated double-stranded RNA (dsRNA) and activates NF-κB, mitogen-activated protein kinase, and IFN regulatory factor (IRF)-3 in a MyD88-independent manner to control viral infection (Matsumoto *et al.*, 2004).

Keratinocytes are the major constituent of the epidermis and the target of viruses, such as herpes simplex virus (Mikloska *et al.*, 1998), human papillomavirus (Cho *et al.*, 2001), and varicella-zoster virus (Nahass *et al.*, 1996). Human keratinocytes express TLR3 both *in vitro* and *in vivo* (Mempel *et al.*, 2003; Tohyama *et al.*, 2005), and cultured keratinocytes produce IFN-α/β followed by macrophage inflammatory protein (MIP)-1α (CCL3) in response to the ligand of TLR3, dsRNA (Tohyama *et al.*, 2005). MIP-1α is chemotactic for monocytes, T lymphocytes, and natural killer cells and is critical for antiviral defense (Menten *et al.*, 2002). Previously, we showed that the lesional epidermis of virus-infected skin expresses MIP-1α, and that dsRNA-treated keratinocytes produce MIP-1α (Tohyama *et al.*, 2005), which indicates that keratinocytes play crucial roles in viral infection. Since chemokines recruit immune cells to attack virus-infected tissues, regulatory mechanisms must exist to avoid aberrant reactions to viral infection, otherwise the innate immune reaction would cause serious tissue damage. However, the negative regulatory mechanism of TLR3 signaling in keratinocytes has not been clarified.

The signal transducers and activators of transcription (STAT) family and its negative regulators, the suppressors of cytokine signaling (SOCS)/cytokine-inducible SH2-containing protein family of proteins, play central roles in regulating cytokine production in various cell types. STATs are crucial molecules for the IFN/cytokine-signaling pathways (Takaoka and Taniguchi, 2003). The SOCS family is induced by STAT activation, and SOCS proteins bind directly to cytokine

[1]*Department of Dermatology, Ehime University School of Medicine, Toon-city, Ehime, Japan and* [2]*Division of Molecular and Cellular Immunology, Medical Institute of Bioregulation, Kyushu University, Fukuoka, Japan*

Correspondence: Dr Koji Sayama, Department of Dermatology, Ehime University School of Medicine, Shitsukawa, Toon-city, Ehime 791-0295, Japan. E-mail: sayama@m.ehime-u.ac.jp

Abbreviations: dsRNA, double-stranded RNA; IRF, IFN regulatory factor; MIP, macrophage inflammatory protein; poly(I:C), polyinosinic-polycytidylic acid; PKR, dsRNA-dependent protein kinase; RIG-I, retinoic acid-inducible gene; RT, reverse transcriptase; SOCS, suppressors of cytokine signaling; STAT, signal transducers and activators of transcription; TLR, Toll-like receptor

Received 29 June 2005; revised 4 January 2006; accepted 17 February 2006; published online 20 April 2006

© 2006 The Society for Investigative Dermatology

receptors or to the catalytic domain of the Janus kinase (JAK) protein, thereby inhibiting the phosphorylation of tyrosine kinase and blocking cytokine signaling (Gadina *et al.*, 2001).

There is some evidence for a link between SOCS and TLR signaling. It has been reported that macrophages from SOCS1-deficient mice exhibit increased LPS sensitivity (Kinjyo *et al.*, 2002), and that the overexpression of SOCS1 impairs TLR triggering (Kinjyo *et al.*, 2002; Baetz *et al.*, 2004). Despite these reports, the inhibitory profile of the SOCS family differs according to cell type and growth conditions. It is not yet known whether or how the SOCS family proteins negatively regulate TLR3 signaling in keratinocytes.

Several IRF molecules are involved in the immune response to viral infection (Sato *et al.*, 2000), among which IRF-3 and IRF-7 regulate the transcription of IFN-α/β genes (Taniguchi *et al.*, 2001). IRF-3 is primarily responsible for the induction of IFN-α/β in the early induction phase of viral infection (Juang *et al.*, 1998). IRF-7 is a short-lived protein, and its expression is dependent on the activation of the transcription factor ISGF3 by type I IFN (Lu *et al.*, 2000). During viral infection, *de novo*-produced IRF-7 is phosphorylated, similarly to IRF-3, which further activates the IFN-α promoter and induces IFN-inducible genes (Marie *et al.*, 1998). Therefore, massive production of IFN-α/β can be achieved through this positive-feedback loop.

Given the importance of IFNs in viral infection and the ability of polyinosinic–polycytidylic acid (poly(I:C)) to induce IFN-α/β production in human keratinocytes, we hypothesized that the STAT family mediates TLR3 signaling and that SOCS family negatively regulates TLR3 signaling in keratinocytes. To support this hypothesis, we utilized adenovirus vectors (Axs) carrying the dominant-negative forms of STAT1, STAT3, and wild-type SOCS1. In this study, we demonstrate for the first time that dsRNA activates the JAK–STAT pathway, which is negatively regulated by SOCS1, in human keratinocytes.

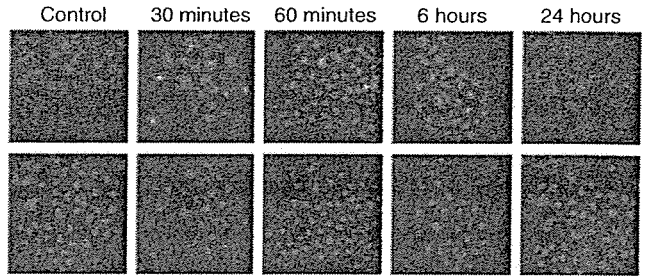

Figure 1. Poly(I:C) induces the nuclear translocation of IRF-3. Poly(I:C)-treated keratinocytes were fixed, and immunofluorescence was performed to detect the nuclear translocation of IRF-3. Green: IRF3 staining; red: 4,6-diamidino-2-phenylindole staining.

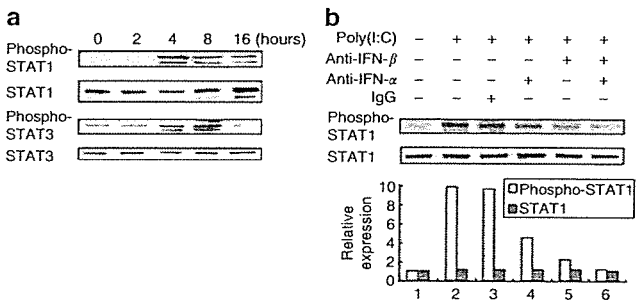

Figure 2. Poly(I:C)-provoked STAT activation is IFN-dependent. (**a**) Keratinocytes were stimulated with poly(I:C), and cell lysates were collected. Immunoblotting was performed with antibodies against STAT1, phospho-STAT1, STAT3, and phospho-STAT3. (**b**) The cultures were neutralized with normal IgG, anti-IFN-α antibody (5 μg/ml), and/or anti-IFN-β antibody (5 μg/ml) for 2 hours before the addition of poly(I:C). The keratinocytes were incubated for another 4 hours, and the cells were collected for evaluation of the STAT1 and phospho-STAT1 levels. The intensity of each band was quantified using the NIH Image software. The relative levels of STAT1 and phospho-STAT1 were normalized against the control, which was designated as one unit.

RESULTS

Poly(I:C) activation of IRF-3 in cultured normal human keratinocytes

We studied whether IRF-3 was activated by poly(I:C) in normal human keratinocytes, since IRF-3 is a key transcription factor for virus-induced IFN expression (Sato *et al.*, 1998, 2000) and poly(I:C)-treated keratinocytes produce IFN-α and IFN-β (Tohyama *et al.*, 2005). We used confocal laser scanning microscopy to investigate the localization of IRF-3 after treatment with poly(I:C). As shown in Figure 1, IRF-3 was located in the cytoplasm of unstimulated keratinocytes. IRF-3 translocated into the nucleus as early as 30 minutes after treatment with poly(I:C), and translocation lasted for 6 hours, which confirms the previous findings in HeLa cells (Iwamura *et al.*, 2001). This result suggests that the activation of IRF-3 mediates poly(I:C)-induced IFN-α/β production in human keratinocytes.

Poly(I:C) activation of the JAK–STAT pathway is dependent upon IFN

We examined whether STATs were phosphorylated in keratinocytes in response to poly(I:C) treatment, as IFN receptors transduce signals via STATs (Takaoka and Taniguchi, 2003). As expected (Figure 2a), poly(I:C) treatment resulted in the phosphorylation of not only STAT1 but also STAT3. We also found that poly(I:C)-induced phosphorylation of STAT1 is dependent upon the expression of IFNs, as pretreatment with neutralizing antibodies against IFN-α or IFN-β significantly inhibited the phosphorylation of STAT1. Furthermore, almost complete blockage of STAT1 phosphorylation was detected when the anti-IFN-α and anti-IFN-β antibodies were added in combination into the culture, whereas the total STAT level was not affected (Figure 2b). Our data also suggest that IFN-β is more important than IFN-α for the activation of STAT1. Blocking the IFN signal also suppressed poly(I:C)-provoked STAT3 phosphorylation (data not shown). Therefore, the poly(I:C)-activated JAK–STAT pathway is type I IFN dependent.

Inhibition of poly(I:C)-induced MIP-1α production by STAT1F but not by STAT3F

Next, we investigated whether the activation of STATs was involved in poly(I:C)-induced MIP-1α production. For this

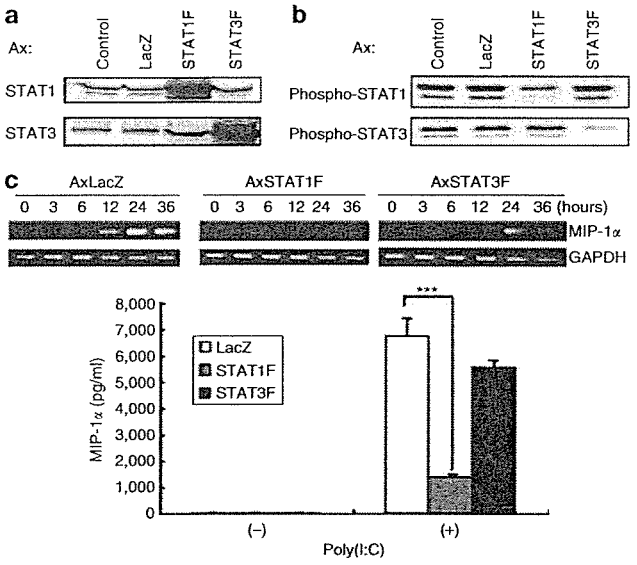

Figure 3. Infection with STAT1F blocks poly(I:C)-induced MIP-1α production. (**a**) Keratinocytes were infected with AxLacZ, AxSTAT1F, and AxSTAT3F for 24 hours. Cell lysates were analyzed for the levels of STAT1 and STAT3 proteins. (**b**) Keratinocytes were infected with AxLacZ, AxSTAT1F, and AxSTAT3F for 24 hours, and the cultures were then stimulated with poly(I:C) for 4 hours. The phosphorylation levels of STAT1 and STAT3 were determined by Western blotting. (**c**) Keratinocytes were infected with AxLacZ, AxSTAT1F, and AxSTAT3F, respectively, and then stimulated with poly(I:C). Total RNA samples were extracted at the indicated times, and the supernatants were collected at 36 hours post-treatment. The production of MIP-1α was examined using real-time RT-PCR and ELISA.

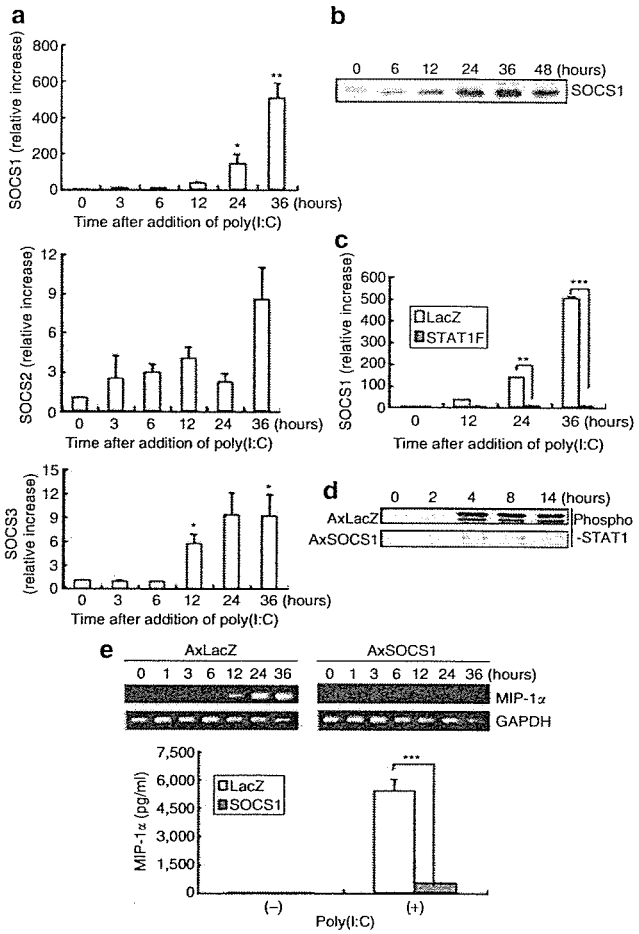

Figure 4. Poly(I:C)-induces SOCS1 expression, and SOCS1 infection inhibits poly(I:C)-induced MIP-1α production. (**a**) Keratinocytes were treated with poly(I:C) for the indicated time periods. The mRNA expression levels of SOCS1, SOCS2, and SOCS3 were examined using real-time RT-PCR. (**b**) Keratinocytes were treated with poly(I:C), and the SOCS1 protein levels were assayed by Western blotting. (**c**) Keratinocytes were infected with AxLacZ or AxSTAT1F for 24 hours before the addition of poly(I:C). Real-time RT-PCR was performed to evaluate the levels of SOCS1 mRNA. (**d**) Keratinocytes were infected with AxLacZ and AxSOCS1 before incubation with poly(I:C). Cell lysates were examined using the phospho-STAT1 antibody. (**e**) Keratinocytes were infected with adenovirus for 24 hours before the addition of poly(I:C). Total RNA samples were extracted, and real-time RT-PCR was performed for MIP-1α mRNA. Supernatants were collected at 36 hours post-treatment, and the MIP-1α protein levels were determined by ELISA.

purpose, we constructed AxSTAT1F and AxSTAT3F. Infection with AxSTAT1F and AxSTAT3F resulted in significant expression of the STAT1 and STAT3 proteins, respectively (Figure 3a), and abolished the poly(I:C)-provoked phosphorylation of STAT1 and STAT3 (Figure 3b), respectively. Therefore, STAT1F and STAT3F specifically inhibit the STAT1 and STAT3 pathways. Poly(I:C) strongly stimulated the production of MIP-1α, which was completely abolished by STAT1F; however, STAT3F had little effect on MIP-1α production (Figure 3c). These data suggest that the STAT1-signaling pathway is essential for poly(I:C)-induced MIP-1α production.

Inhibition of poly(I:C)-induced MIP-1α production by SOCS1

The expression of SOCS1–3 in poly(I:C)-treated keratinocytes was examined by real-time reverse transcriptase (RT)-PCR. The expression of SOCS1 mRNA was enhanced 150-fold at 24 hours and more than 400-fold at 36 hours, compared with the control level at 0 hour; the level of SOCS2 mRNA was increased slightly after 36 hours, and SOCS3 expression was increased several-fold after 12 hours (Figure 4a). Western blot analysis confirmed the induction of SOCS1 (Figure 4b), which is certainly dependent upon the activation of STAT1 (Figure 4c). It has been reported that SOCS1 and SOCS3 inhibit IFN-mediated antiviral activities and that the inhibitory activity of SOCS3 toward STAT1 activation is weaker than that exhibited by SOCS1 (Song and Shuai, 1998). Therefore, we investigated the effect of SOCS1 on poly(I:C)-induced MIP-1α production.

As shown in Figure 4d, the expression of SOCS1 virtually abolished poly(I:C)-induced STAT1 phosphorylation. Furthermore, SOCS1 almost completely blocked poly(I:C)-induced MIP-1α production (Figure 4e). Taken together, these results suggest that the expression of SOCS1 is dependent upon the activation of STAT1, and that SOCS1 negatively regulates poly(I:C)-provoked MIP-1α production by inhibiting STAT1 phosphorylation.

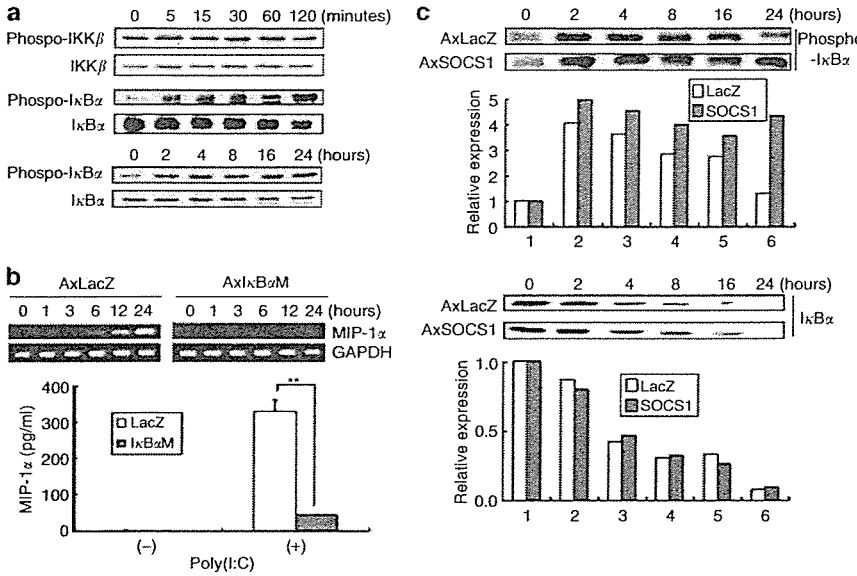

Figure 5. The activation of NF-κB regulates MIP-1α production, but SOCS1 does not affect the NF-κB signal. (a) Poly(I:C) activates the NF-κB signal. Keratinocytes were treated with poly(I:C), and cell lysates were prepared. Immunoblotting was performed with antibodies directed against IKKβ, phospho-IKKβ, IκBα, and phospho-IκBα. (**b**) Infection with IκBαM suppresses poly(I:C)-induced MIP-1α production. Keratinocytes were infected with AxLacZ or AxIκBαM for 24 hours, and the cultures were stimulated with poly(I:C). RNA samples were collected at the indicated times, and supernatants were collected at 36 hours post-treatment. The mRNA and protein levels of MIP-1α were measured. (**c**) SOCS1 does not inhibit the phosphorylation of IκBα. Keratinocytes were infected with AxLacZ and AxSOCS1 for 24 hours before the addition of poly(I:C). Cell lysates were prepared, and Western blotting was performed with antibodies directed against phospho-IκBα and IκBα. The graph is constructed as described in Figure 2b.

Involvement of NF-κB in poly(I:C)-induced MIP-1α production

TLR signaling phosphorylates IκBα and activates the NF-κB signal (Alexopoulou *et al.*, 2001). The activation of the NF-κB signal was detected in poly(I:C)-treated keratinocytes (Figure 5a). The promoter for the gene that encodes MIP-1α contains several NF-κB-binding sites, and NF-κB has been demonstrated to activate MIP-1α transcription in response to cytokines (Guo *et al.*, 2003). Therefore, we studied whether NF-κB was involved in poly(I:C)-provoked MIP-1α production. We introduced the Axs that carries a dominant-negative form of IκBα (IκBαM) to block NF-κB signaling (Dai *et al.*, 2004a). As shown in Figure 5b, the production of MIP-1α was suppressed by IκBαM.

NF-κB is not involved in the inhibition of poly(I:C)-induced MIP-1α production by SOCS1

As SOCS1 has been shown to function as a negative-feedback regulator of TLR4 by suppressing LPS-provoked IκBα phosphorylation and STAT activation in macrophages (Kinjyo *et al.*, 2002; Kimura *et al.*, 2004), we investigated whether the inhibitory effect of SOCS1 on poly(I:C)-induced MIP-1α production was attributable to the inhibition of IκBα phosphorylation. Unexpectedly, infection with AxSOCS1 showed no effect on the level of total IκBα but slightly increased the phosphorylation of IκBα (Figure 5c). This outcome may be explained by the possibility that the inhibition of SOCS1, as a negative regulator for the indirect or secondary effect of TLR3 signaling, benefits the activation of direct signals provoked by dsRNA (Sen and Sarkar, 2005). Neither infection with STAT1F nor blocking of the IFN signal affected the phosphorylation of IκBα (data not shown). Therefore, although NF-κB is involved in MIP-1α production, the inhibition of MIP-1α production by SOCS1 does not occur via the NF-κB signal.

Regulation of poly(I:C)-induced TLR3 expression by the STAT1–SOCS1 pathway

As described previously (Tanabe *et al.*, 2003; Tohyama *et al.*, 2005), type I IFNs are required for poly(I:C)-induced TLR3 upregulation (Figure 6a). Thus, we investigated whether the SOCS1–STAT1 pathway regulates TLR3 expression in poly(I:C)-treated keratinocytes. STAT1F completely abolished the induction of TLR3 mRNA, while STAT3F also inhibited TLR3 expression, albeit less efficiently than STAT1F (Figure 6b). Moreover, SOCS1 expression significantly reduced poly(I:C)-induced TLR3 mRNA expression (Figure 6c). These data indicate that the induction of TLR3 expression by poly(I:C) is also regulated by the STAT1–SOCS1 pathway in keratinocytes.

Inhibition of poly(I:C)-induced IRF-7 expression by SOCS1

Although the IRF-7 protein is undetectable in normal cells, treatment with type I IFNs or viral infection induces the accumulation of IRF-7 (Taniguchi and Takaoka, 2002). The IRF-7 mRNA level in the keratinocytes increased beginning 6 hours post-treatment with poly(I:C); this induction process was dependent upon the type I IFN signal (Ousman *et al.*, 2005), as evidenced by the suppression of IRF-7 expression

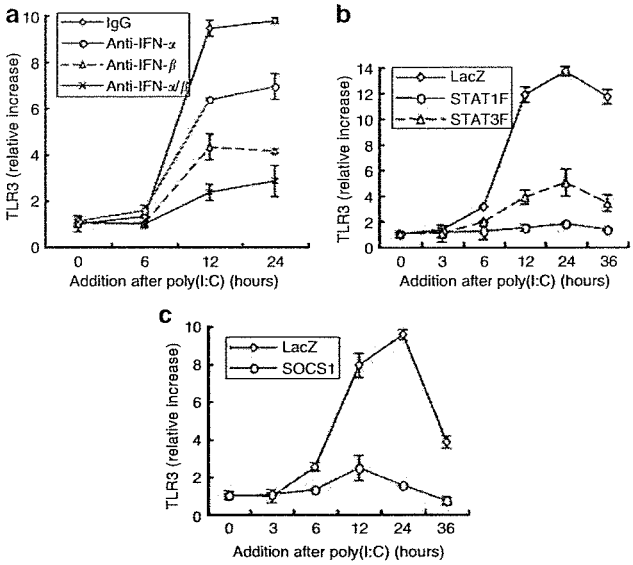

Figure 6. STAT1F and SOCS1 inhibit poly(I:C)-induced TLR3. (a) Keratinocytes were pretreated with normal IgG or neutralizing antibody against type I IFN for 2 hours before the addition of poly(I:C). (b) The protocols for keratinocyte treatment and total cellular RNA preparation were as described in Figure 3c. (c) The protocols for keratinocyte treatment and total cellular RNA preparation were as described in Figure 4e. The expression of TLR3 mRNA was determined by real-time RT-PCR.

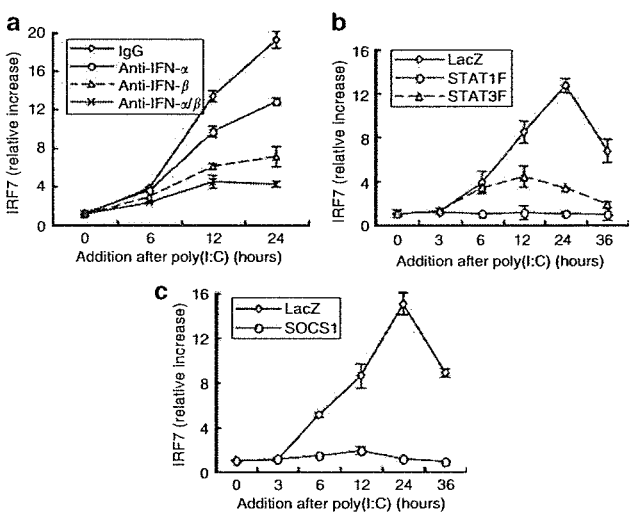

Figure 7. STAT1F and SOCS1 inhibit poly(I:C)-induced IRF-7. The samples described in Figure 6 were used for the detection of IRF-7 mRNA by real-time RT-PCR. (a) The samples were same as Figure 6a. (b) The samples described in Figure 6b were used. (c) RNA samples were prepared as described in Figure 4e. The expressions of IRF-7 mRNA were detected in real time RT-PCR.

by neutralizing antibody against type I IFNs (Figure 7a). STAT1F completely blocked poly(I:C)-induced IRF-7 mRNA expression, whereas STAT3F partially suppressed its expression (Figure 7b). SOCS1 also significantly inhibited IRF-7 expression (Figure 7c). Therefore, activation of the STAT1–SOCS1 pathway is an essential step in this process.

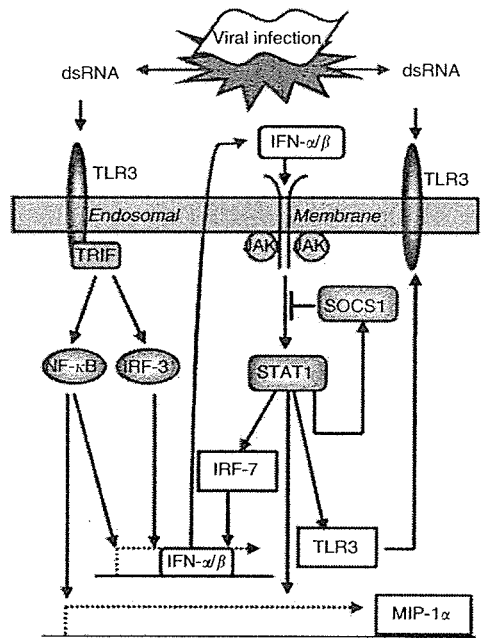

Figure 8. Regulation of dsRNA-provoked innate immune reactions by the STAT1–SOCS1 pathway in normal human keratinocytes. After infection with virus or treatment with dsRNA, the IRF-3, and NF-κB signals are activated, which results in IFN-α/β production. The *de novo*-expressed IFNs stimulate MIP-1α expression by activating the JAK–STAT pathway, which also increases the transcription of the SOCS family members, TLR3, and IRF-7. TLR3 and IRF-7 promote signal amplification, while SOCS1 inhibits STAT1-dependent TLR3, IRF-7, and MIP-1α production by blocking the JAK–STAT1 pathway. Thus, SOCS1 negatively regulates the immune responses of keratinocytes to dsRNA during viral skin infection.

DISCUSSION

Keratinocytes, which are the primary target of viral infections of the skin, are likely to play a pivotal role in virus-induced skin inflammation. Figure 8 summarizes the intracellular signaling mechanisms of the dsRNA-provoked innate immune responses of normal human keratinocytes. Initially, dsRNA enhances IFN-α/β production via TLR3-activated IRF-3 and NF-κB. IFNs activate the JAK–STAT pathway, which results in the expression of genes related to antiviral function. The activation of STAT1 by IFNs not only induces chemokine production, but also results in the expression of IRF-7 and TLR3, thus amplifying the dsRNA-provoked reaction in a positive-feedback manner during viral infection. However, SOCS1, which is another inducible gene, not only blocks STAT1 activation but also inhibits STAT1-dependent TLR3, IRF-7, and MIP-1α. The SOCS1 negative-feedback mechanism for the STAT activation pathway probably impairs autocrine secondary signaling via type I IFN, thereby avoiding exaggerated reactions and regulating the antiviral immune response to viral infection of the skin. This is the first report to indicate that the SOCS–STAT pathway regulates MIP-1α production in dsRNA-stimulated keratinocytes.

Since the induction of SOCS was initially attributed to the JAK/STAT pathways, SOCS has generally been thought to act on JAK/STAT cascades. However, this idea has recently been

challenged by the finding that SOCS−/− mice show enhanced responses to LPS, with strongly enhanced phosphorylation of IκBα, p38, and JNK (Kinjyo *et al.*, 2002). Moreover, overexpression of SOCS1 suppresses LPS-induced NF-κB activation, a process through which SOCS1 inhibits TLR4-specific cytokine induction (Kinjyo *et al.*, 2002). However, two other groups have presented contrasting data (Baetz *et al.*, 2004; Gingras *et al.*, 2004), which are consistent with our observations that SOCS1 has no negative effects on the poly(I:C)-stimulated rapid activation of NF-κB signaling. In this study, we show the almost complete inhibition by SOCS1 of STAT1 activation in TLR3 signaling, and demonstrate that SOCS1 inhibits MIP-1α expression by disabling the STAT1 signal and not the NF-κB signal, although the NF-κB signal is also required for MIP-1α production.

The continuous expression of IRF-7 through type I IFN results in the amplification of the IFN signal, which plays an important role in ensuring a robust immune response during viral infection. In this study, we found that poly(I:C) induces IRF-7 expression, which is dependent upon type I IFN-stimulated STAT1 activation. It has been reported that virus-induced regulated upon activation, normal T-cell expressed and secreted (RANTES) gene expression is blocked in airway epithelial cells through the inhibition of IRF-7 expression (Casola *et al.*, 2001). We propose that SOCS1 partially regulates MIP-1α expression by inhibiting IRF-7. SOCS1 may inhibit the JAK/STAT-dependent autocrine and paracrine amplification loops, for example, additional activation via type I IFNs. Based on these findings, we suggest that the STAT–SOCS pathway plays a role in avoiding the unnecessary amplification of the immune response and in keeping host defenses balanced by regulating the activities of the IRF family and TLR3.

The dsRNA-dependent protein kinase (PKR) has been implicated in dsRNA-activated signaling (Chu *et al.*, 1999). PKR exists in most cell types and *trans*-autophosphorylates in response to poly(I:C). PKR has been shown to regulate poly(I:C)-induced tumor necrosis factor-α (Meusel *et al.*, 2002). However, PKR is not the kinase responsible for phosphorylating and activating IRF-3 (Chu *et al.*, 1999). Furthermore, we did not detect any notable level of phosphorylated PKR in the poly(I:C)-treated keratinocytes (data not shown). All of these events support the notion that the poly(I:C)-stimulated signal in keratinocytes is independent of PKR.

The existence of a viral sensor other than TLR3 has been proposed (Levy and Marie, 2004). The RNA helicase retinoic acid-inducible gene (RIG-I) probably serves as this type of sensor, as RIG-I has been demonstrated to activate IRF-3 and induce IFN-β production (Levy and Marie, 2004; Yoneyama *et al.*, 2004). It has been reported that the responses to viral infection or to intracellular dsRNA are reduced in the absence of RIG-I, whereas the extracellular dsRNA-stimulated responses mediated by TLR3 remain intact (Yoneyama *et al.*, 2004). Both TLR3 and RIG-I sense the *in vivo* immune responses to viruses. It is possible that MIP-1α production and JAK–STAT activation in virus-infected keratinocytes are mediated partially via RIG-I. Therefore, the involvement of RIG-I in the virus-induced innate immune responses of keratinocytes should be clarified.

Our investigations suggest that SOCS1 mainly suppresses the indirect effects of the dsRNA signal and negatively regulates the viral immune response to avoid exaggerated reactions. Therefore, the STAT–SOCS1 pathway plays a critical role in the maintenance of homeostasis in the innate immune system of the skin.

MATERIALS AND METHODS

Reagents

Normal IgG, as well as the anti-IFN-α and anti-IFN-β antibodies were purchased from R&D Systems (Minneapolis, MN), and the anti-IRF-3 antibody was purchased from Santa Cruz Biotechnology (Santa Cruz, CA). The remaining antibodies used in this study were obtained from Cell Signaling Technology (Beverly, MA).

Cell culturing and treatment

Normal human keratinocytes were cultured in MCDB153 medium that was supplemented with insulin (5 μg/ml), hydrocortisone (5×10^{-7} M), ethanolamine (0.1 mM), phosphoethanolamine (0.1 mM), bovine hypothalamic extract (50 μg/ml), and Ca^{2+} (0.03 mM), as described previously (Shirakata *et al.*, 2004). Cells that had been passaged four times were used in the experiments, and subconfluent keratinocyte cultures were treated with 100 ng/ml of poly(I:C) (Amersham Biosciences Corp., Piscataway, NJ) for a predetermined period of time. The study was conducted according to the Declaration of Helsinki Principles. All of the procedures that involved human subjects received prior approval from the Ethical Committee of Ehime University School of Medicine, and all the subjects provided written informed consent.

Adenovirus construction and infection

The cosmid cassette pAxCAw and the parental virus Ad5-dlX were kind gifts from Dr Izumu Saito (Tokyo University, Japan) (Miyake *et al.*, 1996). The full-length coding regions of STAT1F, STAT3F, and SOCS1 cDNA were subcloned into pAxCAw. The STAT1F and STAT3F genes encode dominant-negative mutant proteins, in which the tyrosine phosphorylation sites have been changed to phenylalanine (Yamasaki *et al.*, 2003). Axs that contained the CA promoter and STAT1F, STAT3F, or SOCS1/JAB were generated using the cosmid cassettes and Ad DNA-TPC method (Miyake *et al.*, 1996). The cosmid DNA was mixed with the *Eco*T221-digested DNA-terminal Ad5–dLX protein complex, which was used to transfect 293 cells. The recombinant viruses were generated through homologous recombination in 293 cells, and the virus stocks were prepared using a standard procedure (Miyake *et al.*, 1996). Concentrated, purified virus stocks were prepared by CsCl gradient centrifugation, and the virus titers were estimated in a plaque formation assay.

Cultured normal human keratinocytes were infected with Ax STAT1F, AxSTAT3F, or AxSOCS1 at a multiplicity of infection of 10, as described previously (Yamasaki *et al.*, 2003), and AxLacZ was used as the control vector. The AxIκBαM vector was constructed and infected into keratinocytes as described previously (Dai *et al.*, 2004a).

Immunofluorescence microscopy

The keratinocytes were seeded on chamber slides. The treated cells were fixed for 5 minutes in methanol:acetone (1:1), and treated with

the anti-IRF-3 antibody overnight at 4°C. After washing with phosphate-buffered saline, the cells were incubated with fluorescein-labeled goat anti-rabbit IgG for 30 minutes at 37°C. 4,6-Diamidino-2-phenylindole staining of the nucleus was also performed. The stained cells were visualized at an original magnification of ×40 under an LSM 510 microscope (Carl Zeiss, Jena, Germany). Images were captured using the LSM 510 software.

RT-PCR

Total RNA samples were isolated using Isogen (Nippon Gene, Tokyo, Japan), and RT-PCR was performed using RT-PCR High Plus (Toyobo, Osaka, Japan) (Dai *et al.*, 2004b). The expression levels of *MIP-1α* and glyceraldehyde-3-phosphate dehydrogenase mRNA were detected using specific primers (primer list: Table S1). The PCR products were sequenced to confirm the accuracy of amplification.

Real-time RT-PCR

Real-time RT-PCR was performed in an ABI PRISM 7700 sequence detector (PE Applied Biosystems, Foster City, CA). The primers and probes for glyceraldehyde-3-phosphate dehydrogenase, *TLR3*, and *IRF-7* were obtained from Applied Biosystems (Norwalk, CT). The primers and probes for members of the human *SOCS* family are shown in Table S2. The RNA analysis was carried out using the TaqMan RT-PCR Master Mix reagents kit (Applied Biosystems, Norwalk, CT) and the quantification of gene expression was performed using the comparative computed tomography method, as described previously (Dai *et al.*, 2004a). The level of target gene expression in the test samples was normalized to the corresponding glyceraldehyde-3-phosphate dehydrogenase level and is reported as the fold difference. In this study, each assay was performed in triplicate, and the factorial change of each sample was normalized against that of the vehicle as one unit.

ELISA

Culture supernatants were collected at the indicated times after treatment and were stored at −70°C until subjected to ELISA. The ELISA kit for MIP-1α was purchased from Endogen (Auburn, MA). ELISA was performed according to the manufacturer's instructions.

Protein preparation and Western blot analysis

The cells were harvested by transfer into extraction buffer that contained 150 mM NaCl, 1% Nonidet P-40, 0.5% deoxycholate, 0.1% SDS, 50 mM Tris-HCl (pH 7.4), and protease inhibitors. Equal amounts of protein were separated by SDS-PAGE electrophoresis and transferred to polyvinylidene difluoride membranes. The analysis was performed using the Vistra ECF kit (Amersham Biosciences, Tokyo, Japan) and a FluorolmageR (Molecular Dynamics, Sunnyvale, CA).

Statistical analyses

In this study, at least three independent experiments were performed, with similar results, and one representative experiment is shown in each of the figures. The quantitative ELISA data and the relative mRNA expression levels detected by real-time RT-PCR are expressed as the mean±SD ($N=3$). Statistical significance was determined by the paired Student's *t*-test. Differences were considered to be statistically significant for $P<0.05$. The levels of statistical significance are indicated as follows in the figures: $^{*}P<0.05$; $^{**}P<0.01$; and $^{***}P<0.001$.

CONFLICT OF INTEREST
The authors state no conflict of interest.

ACKNOWLEDGMENTS
We thank Teruko Tsuda and Eriko Tan for technical assistance.

SUPPLEMENTARY MATERIAL

Table S1. Primer pairs for RT-PCR.

Table S2. Primer and probe list for real time RT-PCR.

REFERENCES

Alexopoulou L, Holt AC, Medzhitov R, Flavell RA (2001) Recognition of double-stranded RNA and activation of NF-kappaB by Toll-like receptor 3. *Nature* 413:732–8

Baetz A, Frey M, Heeg K, Dalpke AH (2004) Suppressor of cytokine signaling (SOCS) proteins indirectly regulate toll-like receptor signaling in innate immune cells. *J Biol Chem* 279:54708–15

Casola A, Burger N, Liu T, Jamaluddin M, Brasier AR, Garofalo RP (2001) Oxidant tone regulates RANTES gene expression in airway epithelial cells infected with respiratory syncytial virus. Role in viral-induced interferon regulatory factor activation. *J Biol Chem* 276:19715–22

Cho YS, Kang JW, Cho M, Cho CW, Lee S, Choe YK *et al.* (2001) Down-modulation of IL-18 expression by human papillomavirus type 16 E6 oncogene via binding to IL-18. *FEBS Letts* 501:139–45

Chu WM, Ostertag D, Li ZW, Chang L, Chen Y, Hu Y *et al.* (1999) JNK2 and IKKbeta are required for activating the innate response to viral infection. *Immunity* 11:721–31

Dai X, Yamasaki K, Shirakata Y, Sayama K, Hashimoto K (2004a) All-*trans*-retinoic acid induces interleukin-8 via the nuclear factor-kappaB and p38 mitogen-activated protein kinase pathways in normal human keratinocytes. *J Invest Dermatol* 123:1078–85

Dai X, Yamasaki K, Yang L, Sayama K, Shirakata Y, Tokumara S *et al.* (2004b) Keratinocyte G2/M growth arrest by 1,25-dihydroxyvitamin D3 is caused by Cdc2 phosphorylation through Wee1 and Myt1 regulation. *J Invest Dermatol* 122:1356–64

Gadina M, Hilton D, Johnston JA, Morinobu A, Lighvani A, Zhou YJ *et al.* (2001) Signaling by type I and II cytokine receptors: ten years after. *Curr Opin Immunol* 13:363–73

Gingras S, Parganas E, de Pauw A, Ihle JN, Murray PJ, Yoshimura A *et al.* (2004) Re-examination of the role of suppressor of cytokine signaling 1 (SOCS1) in the regulation of toll-like receptor signaling. *J Biol Chem* 279:54702–7

Guo CJ, Douglas SD, Lai JP, Pleasure DE, Li Y, William S *et al.* (2003) Interleukin-1beta stimulates macrophage inflammatory protein-1alpha and -1beta expression in human neuronal cells (NT2-N). *J Neurochem* 84:997–1005

Iwamura T, Yoneyama M, Yamaguchi K, Suhara W, Mori W, Shiota K *et al.* (2001) Induction of IRF-3/-7 kinase and NF-kappaB in response to double-stranded RNA and virus infection: common and unique pathways. *Genes Cells* 6:375–88

Juang YT, Lowther W, Kellum M, Au WC, Lin R, Hiscott J *et al.* (1998) Primary activation of interferon A and interferon B gene transcription by interferon regulatory factor 3. *Proc Natl Acad Sci USA* 95:9837–42

Kimura A, Naka T, Nagata S, Kawase I, Kishimoto T (2004) SOCS-1 suppresses TNF-alpha-induced apoptosis through the regulation of Jak activation. *Int Immunol* 16:991–9

Kinjyo I, Hanada T, Inagaki-Ohara K, Mori H, Aki D, Ohishi M *et al.* (2002) SOCS1/JAB is a negative regulator of LPS-induced macrophage activation. *Immunity* 17:583–91

Levy DE, Marie IJ (2004) RIGging an antiviral defense – it's in the CARDs. *Nat Immunol* 5:699–701

Lu R, Au WC, Yeow WS, Hageman N, Pitha PM (2000) Regulation of the promoter activity of interferon regulatory factor-7 gene. Activation by interferon and silencing by hypermethylation. *J Biol Chem* 275:31805–12

Marie I, Durbin JE, Levy DE (1998) Differential viral induction of distinct interferon-alpha genes by positive feedback through interferon regulatory factor-7. *EMBO J* 17:6660–9

Matsumoto M, Funami K, Oshiumi H, Seya T (2004) Toll-like receptor 3: a link between toll-like receptor, interferon and viruses. *Microbiol Immunol* 48:147–54

Mempel M, Voelcker V, Kollisch G, Plank C, Rad R, Gerhard M *et al.* (2003) Toll-like receptor expression in human keratinocytes: nuclear factor-kappaB controlled gene activation by *Staphylococcus aureus* is toll-like receptor 2 but not toll-like receptor 4 or platelet activating factor receptor dependent. *J Invest Dermatol* 121:1389–96

Menten P, Wuyts A, Van Damme J (2002) Macrophage inflammatory protein-1. *Cytokine Growth Factor Rev* 13:455–81

Meusel TR, Kehoe KE, Imani F (2002) Protein kinase R regulates double-stranded RNA induction of TNF-alpha but not IL-1 beta mRNA in human epithelial cells. *J Immunol* 168:6429–35

Mikloska Z, Danis VA, Adams S, Lloyd AR, Adrian DL, Cunningham AL *et al.* (1998) *In vivo* production of cytokines and beta (C-C) chemokines in human recurrent herpes simplex lesions – do herpes simplex virus-infected keratinocytes contribute to their production? *J Infect Dis* 177:827–38

Miyake S, Makimura M, Kanegae Y, Harada S, Sato Y, Takamori K *et al.* (1996) Efficient generation of recombinant adenoviruses using adenovirus DNA-terminal protein complex and a cosmid bearing the full-length virus genome. *Proc Natl Acad Sci USA* 93:1320–4

Nahass GT, Penneys NS, Leonardi CL (1996) Interface dermatitis in acute varicella-zoster virus infection: demonstration of varicella-zoster virus DNA in keratinocytes by *in situ* polymerase chain reaction. *Br J Dermatol* 135:150–1

Ousman SS, Wang J, Campbell IL (2005) Differential regulation of interferon regulatory factor (IRF)-7 and IRF-9 gene expression in the central nervous system during viral infection. *J Virol* 79:7514–27

Sato M, Suemori H, Hata N, Asagiri M, Ogasawara K, Nakao K *et al.* (2000) Distinct and essential roles of transcription factors IRF-3 and IRF-7 in response to viruses for IFN-alpha/beta gene induction. *Immunity* 13:539–48

Sato M, Tanaka N, Hata N, Oda E, Taniguchi T (1998) Involvement of the IRF family transcription factor IRF-3 in virus-induced activation of the IFN-beta gene. *FEBS Letts* 425:112–6

Sen GC, Sarkar SN (2005) Transcriptional signaling by double-stranded RNA: role of TLR3. *Cytokine Growth Factor Rev* 16:1–14

Shirakata Y, Ueno H, Hanakawa Y, Kameda K, Yamasaki K, Tokumaru S *et al.* (2004) TGF-beta is not involved in early phase growth inhibition of keratinocytes by 1alpha,25$(OH)_2$ vitamin D3. *J Dermatol Sci* 36:41–50

Song MM, Shuai K (1998) The suppressor of cytokine signaling (SOCS) 1 and SOCS3 but not SOCS2 proteins inhibit interferon-mediated antiviral and antiproliferative activities. *J Biol Chem* 273:35056–62

Takaoka A, Taniguchi T (2003) New aspects of IFN-alpha/beta signalling in immunity, oncogenesis and bone metabolism. *Cancer Sci* 94:405–11

Takeda K, Kaisho T, Akira S (2003) Toll-like receptors. *Annu Rev Immunol* 21:335–76

Tanabe M, Kurita-Taniguchi M, Takeuchi K, Takeda M, Ayata M, Ogura H *et al.* (2003) Mechanism of up-regulation of human Toll-like receptor 3 secondary to infection of measles virus-attenuated strains. *Biochem Biophys Res Commun* 311:39–48

Taniguchi T, Ogasawara K, Takaoka A, Taraka N (2001) IRF family of transcription factors as regulators of host defense. *Annu Rev Immunol* 19: 623–55

Taniguchi T, Takaoka A (2002) The interferon-alpha/beta system in antiviral responses: a multimodal machinery of gene regulation by the IRF family of transcription factors. *Curr Opin Immunol* 14:111–6

Tohyama M, Dai X, Sayama K, Yamasaki K, Shirakata Y, Hanakawa Y *et al.* (2005) dsRNA-mediated innate immunity of epidermal keratinocytes. *Biochem Biophys Res Commun* 335:505–11

Yamasaki K, Hanakawa Y, Tokumaru S, Shirakata Y, Sayama K, Hanada T *et al.* (2003) Suppressor of cytokine signaling 1/JAB and suppressor of cytokine signaling 3/cytokine-inducible SH2-containing protein 3 negatively regulate the signal transducers and activators of transcription signaling pathway in normal human epidermal keratinocytes. *J Invest Dermatol* 120:571–80

Yoneyama M, Kikuchi M, Natsukawa T, Shinobu N, Imaizumi T, Miyagishi M *et al.* (2004) The RNA helicase RIG-I has an essential function in double-stranded RNA-induced innate antiviral responses. *Nat Immunol* 5: 730–7

THE JOURNAL OF BIOLOGICAL CHEMISTRY VOL. 281, NO. 19, pp. 13209–13216, May 12, 2006
© 2006 by The American Society for Biochemistry and Molecular Biology, Inc. Printed in the U.S.A.

A Novel Function of Angiotensin II in Skin Wound Healing

INDUCTION OF FIBROBLAST AND KERATINOCYTE MIGRATION BY ANGIOTENSIN II VIA HEPARIN-BINDING EPIDERMAL GROWTH FACTOR (EGF)-LIKE GROWTH FACTOR-MEDIATED EGF RECEPTOR TRANSACTIVATION

Received for publication, September 6, 2005, and in revised form, March 16, 2006 Published, JBC Papers in Press, March 16, 2006, DOI 10.1074/jbc.M509771200

Yoko Yahata[‡1], Yuji Shirakata[‡1,2], Sho Tokumaru[‡], Lujun Yang[‡], Xiuju Dai[‡], Mikiko Tohyama[‡], Teruko Tsuda[‡], Koji Sayama[‡], Masaru Iwai[§], Masatsugu Horiuchi[§], and Koji Hashimoto[‡]

From the [‡]Department of Dermatology and the [§]Division of Medical Biochemistry and Cardiovascular Biology, Ehime University School of Medicine, Shitsukawa, Toon, Ehime 791-0295, Japan

The role of angiotensin II (Ang II) in the control of systemic blood pressure and volume homeostasis is well known and has been extensively studied. Recently, Ang II was suggested to also have a function in skin wound healing. In the present study, the *in vivo* function of Ang II in skin wound healing was investigated using Ang II type 1 receptor (AT1R) knock-out mice. Wound healing in these mice was found to be markedly delayed. Keratinocytes and fibroblasts play important roles in wound healing, and thus the effect of Ang II on the migration of these cells was examined. Ang II stimulated keratinocyte and fibroblast migration in a dose-dependent manner. It has been reported that G protein-coupled receptor (GPCR) activation induces epidermal growth factor (EGF) receptor (EGFR) transactivation through the shedding of heparin-binding EGF-like growth factor (HB-EGF). As AT1R is a GPCR, it was hypothesized that Ang II-induced keratinocyte and fibroblast migration is mediated by EGFR transactivation. Ang II induced EGFR phosphorylation, which was inhibited by an AT1R antagonist, HB-EGF neutralizing antibody, and an HB-EGF antagonist in both keratinocytes and in fibroblasts. Moreover, Ang II-induced migration of keratinocytes and fibroblasts was also prevented by these inhibitors. Taken together, these findings clearly demonstrate, for the first time, that Ang II plays an important role in skin wound healing and that it functions by accelerating keratinocyte and fibroblast migration in a process mediated by HB-EGF shedding.

Cutaneous wound healing requires precise coordination of epithelialization, dermal repair, and angiogenesis (1). In turn, epithelialization is ultimately dependent on the migratory, proliferative, and differentiation abilities of keratinocytes, while dermal repair requires the production of extracellular matrix by fibroblasts. The growth and differentiation of these two cell types are regulated by several different growth factors (2).

The vasoactive octapeptide angiotensin II (Ang II)[3] has a well described role in the control of systemic blood pressure and volume homeostasis. In the rat, both cardiac and skin fibroblasts express Ang II receptors, which have been shown to be involved in cell growth and the activation of second messenger pathways, such as the mobilization of intracellular calcium (3, 4). In addition, Ang II was shown to act as a mitogen for smooth muscle cells, fibroblasts, and endothelial cells (5–10). Mammalian cells express two types of Ang II receptors, Ang II type 1 receptor (AT1R) and Ang II type 2 receptor (AT2R) (11). Most of the known biological effects of Ang II are mediated through AT1R, a G protein-coupled receptor (GPCR) that is expressed in a wide variety of cells and tissues. In mouse, there are two isoforms of AT1R, AT1aR and AT1bR. AT1R has been shown to mediate mitogenesis in cardiac fibroblasts and vascular smooth muscle cells (12, 13), whereas in fibroblasts, the activation of AT2R has two opposing effects, inhibition of cell growth (14, 15) and promotion of apoptosis (16). Thus, the balance between the expressions of these two receptor types may be crucial in determining the response to Ang II. The integral role of Ang II in regulating systemic blood pressure and volume homeostasis is well known and has been extensively studied. In the present study, we show that Ang II is also involved in wound repair.

Recent investigations demonstrated that the stimulation of GPCR induces shedding of epidermal growth factors (EGF) via the activation of a disintegrin and metalloprotease (ADAM), followed by transactivation of the EGF receptor (EGFR). HB-EGF, an EGF family member, is thought to play a major role in this process. HB-EGF is a single transmembrane-spanning protein that is proteolytically cleaved at a juxtamembrane site, leading to the shedding of soluble EGFR ligand, which in turn activates the EGFR in an autocrine/paracrine manner (17).

The physiological functions as well as the underlying cellular and molecular mechanisms of AT1R in the cardiovascular system have been the focus of many studies, whereas the role of Ang II receptors in skin is not well established. It has been reported that adult rat skin contains predominantly AT1R (18) and that Ang II accelerates the closure of thermal injuries and full-thickness dermal lesions. Both of these responses are associated with the enhancement of several physiological processes necessary for skin wound repair, such as the proliferation of keratinocytes and the production of extracellular matrix (19–21).

As AT1R is a GPCR and as HB-EGF plays an important role in skin wound healing, we investigated the involvement of Ang II-AT1R in skin wound healing. Our results clearly demonstrated that Ang II participates in skin wound healing by accelerating both keratinocyte and fibroblast migration in a process mediated by HB-EGF shedding.

EXPERIMENTAL PROCEDURES

Cell Culture and Reagents—Normal human epidermal keratinocytes were cultured in MCDB 153 type II medium as described previously (22). Keratinocytes in their fourth passage were used in this study. Nor-

* This work was supported in part by a grant for scientific research from the Ministry of Education, Culture, Sports, Science, and Technology of Japan and by a grant for Research on Specific Disease from the Ministry of Health, Labor, and Welfare of Japan. The costs of publication of this article were defrayed in part by the payment of page charges. This article must therefore be hereby marked "*advertisement*" in accordance with 18 U.S.C. Section 1734 solely to indicate this fact.

[1] These authors contributed equally to this work.
[2] To whom correspondence should be addressed. Tel.: 81-89-960-5350; Fax: 81-89-960-5352; E-mail: shirakat@m.ehime-u.ac.jp.

[3] The abbreviations used are: Ang II, angiotensin II; AT1R, angiotensin II type 1 receptor; AT2R, angiotensin II type 2 receptor; TGF-β, transforming growth factor-β; PDGF, platelet-derived growth factor; EGF, epidermal growth factor; EGFR, epidermal growth factor receptor; HB-EGF, heparin-binding EGF-like growth factor; GPCR, G protein-coupled receptor; DMEM, Dulbecco's modified Eagle's medium; FCS, fetal calf serum; RT, reverse transcription; MMP, matrix metalloproteinase.

The Journal of Biological Chemistry

Downloaded from www.jbc.org at EHIME UNIVERSITY on February 27, 2007